Mohd Mansor, MS, Raja, S, Yusof, F, Muhamad, MR, Manurung, YHP, Adenan, MS, Hussein, NIS and Ren, J

Integrated approach to Wire Arc Additive Manufacturing (WAAM) optimization: Harnessing the synergy of process parameters and deposition strategies

Journal of Materials Research and Technology 30 (2024) 2478–2499

Contents lists available at ScienceDirect

Journal of Materials Research and Technology

journal homepage: www.elsevier.com/locate/jmrt

Integrated approach to Wire Arc Additive Manufacturing (WAAM) optimization: Harnessing the synergy of process parameters and deposition strategies

Muhammad Safwan Mohd Mansor [a,b], Sufian Raja [a,b], Farazila Yusof [a,b,c,*], Mohd Ridha Muhamad [a,b], Yupiter HP. Manurung [d], Mohd Shahriman Adenan [d], Nur Izan Syahriah Hussein [e], James Ren [f]

[a] Department of Mechanical Engineering, Faculty of Engineering, University of Malaya, 50603, Kuala Lumpur, Malaysia
[b] Centre of Advanced Manufacturing and Material Processing (AMMP Centre), University of Malaya, 50603, Kuala Lumpur, Malaysia
[c] Centre for Foundation Studies in Science (PASUM), University of Malaya, 50603, Kuala Lumpur, Malaysia
[d] Smart Manufacturing Research Institute (SMRI), MARA University of Technology (UITM), 40450, Shah Alam, Selangor, Malaysia
[e] Faculty of Manufacturing Engineering, Technical University of Malaysia (UTeM), Hang Tuah Jaya, 76100, Durian Tunggal, Melaka, Malaysia
[f] Faculty of Engineering and Technology, James Parsons Building, Liverpool John Moore's University, 3 Byrom St, Liverpool, L3 3AF, United Kingdom

A R T I C L E I N F O

Keywords:
Wire-Arc Additive Manufacturing
Process parameter optimization
Near-net-shape
WAAM deposition strategy
Statistical analysis tool

A B S T R A C T

The flexibility of Additive Manufacturing (AM) technologies in the metal 3D printing process has gained significant attention in research and industry, which allows for fabricating complicated and intricate Near-Net-Shape (NNS) geometry designs. The achievement of desired characteristics in Wire-Arc Additive Manufactured (WAAM) components is primarily contingent upon the careful selection and precise control of significant processing variables, including bead deposition strategy, wire materials, type of heat source, wire feed speed, and the application of shielding gas. As a result, optimizing these most significant process parameters has improved, producing higher-quality WAAM-manufactured components. Consequently, this has contributed to the overall rise in the method's popularity and many applications. This article aims to provide an overview of the wire deposition strategy and the optimization of process parameters in WAAM. The optimization of numerous wire deposition techniques and process parameters in the WAAM method, which is required to manufacture high-quality additively manufactured metal parts, is summarised. The WAAM optimization algorithm, in addition to anticipate technological developments, has been proposed. Subsequently, a discussion ensues regarding the potential for WAAM optimization within the swiftly growing domain of WAAM. In the end, conclusions have been derived from the reviewed research work.

1. Introduction

Additive manufacturing (AM) has been widely discussed by engineers and researchers as a way to lead the manufacturing industry in producing medium-to-large scale Near-Net-Shape (NNS) components more quickly, economically, and with less waste [1]. Due to the multi-purpose capabilities within AM, many manufacturing industries have shifted towards this technology instead of subtractive manufacturing (SM) [1,2]. Furthermore, AM can manufacture relatively complex geometries better than SM due to how it is revolutionized for various types of materials [3]. AM of NNS metal components comprises of powder-based and wire-based technology [1]. Fig. 1 show types of AM process based on the raw materials used and their respective technologies found throughout recent research developments.

AM techniques can be classified into powder-based and wire-based processes based on the type of energy source utilised for feedstock distributions [4–7]. Powder-based additive manufacturing offers benefits such as a relatively small pool, a concentrated energy source, and precise depositing. Heterogeneous metallic components with complicated geometries can be manufactured by adjusting the powder composition proportions of the feedstock materials in an immediate fashion. This ability demonstrates the wide-ranging practical utility of powder-based

* Corresponding author. Department of Mechanical Engineering, Faculty of Engineering, University of Malaya, 50603, Kuala Lumpur, Malaysia.
E-mail address: farazila@um.edu.my (F. Yusof).

https://doi.org/10.1016/j.jmrt.2024.03.170
Received 20 December 2023; Received in revised form 20 March 2024; Accepted 23 March 2024
Available online 26 March 2024

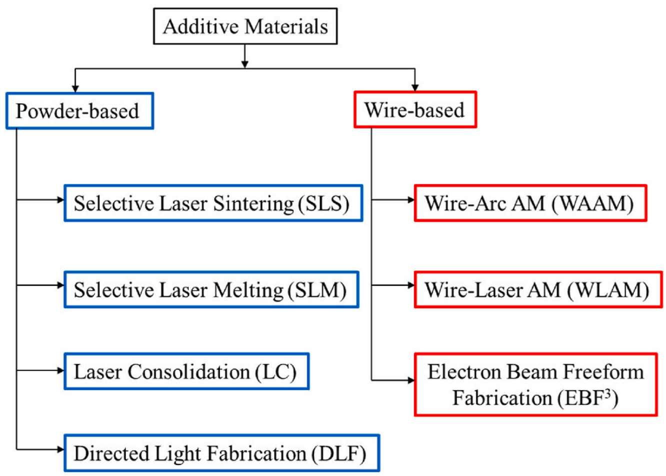

Fig. 1. Additive materials classification based on type of raw materials and respective technologies.

additive manufacturing technology, encompassing applicability in the biomedical, oil and gas fields. Challenges in achieving dense components include the substantial expense of powder materials, limited depositing efficiency, low utilization rates, porosity and lack of fusion [8–11].

The wire extracted from the feedstock is introduced promptly into the molten pool produced by the heat source, enabling the wire material to melt either in a shielding gas environment or in a vacuum state in a layer-by-layer fashion in wire-based additive manufacturing [12]. Wire-based additive manufacturing methods can produce wholeheartedly dense parts or components with precise control over microstructural characteristics [5,13,14]. Wire-based additive manufacturing methods have enabled the cost-effective production of profound metallic parts with moderate complexity [15]. The primary limitations of the Wire-based Additive Manufacturing technology are low precision resolution and an average surface finish. Components manufactured through this process require finishing on the surface using CNC machines [16,17].

WAAM is one of the most prevalent AM processes for 3D metal printing and offers several advantages. WAAM is more effective at making large-scale components than other AM technologies because it uses low-cost materials and is efficient and productive [18]. Additionally, metal-wire has many advantages over powder-feed technology. The cost of metal wire is around 10% of metal powder. Thus, the WAAM method performs well with high deposition rate at a cheap cost, making it ideal for fabricating large components with an acceptable buy-to-fly ratio from costly metals [19,20]. Due to powder-feed technology's poor deposition rate of 10 g/min [21], wire-feed is favoured and widely employed in the industry. Table 1 summarizes some of the WAAM process applications concerning the welding heat source employed by researchers.

There are four primary heat sources commonly used for the WAAM process to melt the wire metals: gas metal arc welding (GMAW), cold metal transfer (CMT), gas tungsten arc welding (GTAW), and plasma arc welding (PAW). GMAW-based WAAM is known for its simple tool path-planning algorithm, user-friendliness, cheaper capital cost, and greater convenience to use than other heat sources [28]. The CMT-based WAAM technique is frequently utilised compared to other WAAM processes due to its high deposition rate, low heat input, little dilution of base metal alloys, controllable structural deformation, and low residual stress accumulation [60–62]. GTAW and PAW-based WAAM use the same method of producing molten pools using non-consumable tungsten electrodes. Unlike GMAW, GTAW and PAW require an external wire feed machine or separate wire feeding system to supply the feed materials [63].

In WAAM process, Wire Feed Speed has a very strong correlation with the speed of deposition rate, which significantly affects the overall quality of the manufactured parts [64]. In addition, according to the research conducted by B. Wu et al. [64], it is possible to achieve consistent and stable metal transfer behaviour in the WAAM process by meticulously controlling the inter-pass temperature and using appropriate localised gas shielding. Meanwhile, Dinovitzer et al. [65] state that the main cause of wire-feeding AM process problems significantly originated from residual stress and distortion formation. It revealed that the WAAM process is a viable wire-feed technology as long as optimal values were selected for the travel speed, wire feed rate, current, and gas flow rate. Controlling process parameters in WAAM has proven difficult to optimize and sustain efficiency [66]. This requires the development of an approach to optimize the manufacture of big near-net shape (NNS) parts by removing or minimising errors in the final product.

Fig. 2 presents the research challenges and future directions for the WAAM process. The deposition strategy and process parameters are crucial in the widespread adoption of WAAM as a high deposition rate and have become the main focus of this review paper. Currently, many methods are employed for optimization, particularly for WAAM process. Due to the very intricate nature of WAAM, it is necessary to delve into diverse topics, including process optimization, deposition strategy, and adaptability of statistical tools.

Several scholarly review articles on the WAAM have been written by researchers, focusing on advanced systems, design, utilization, real-time monitoring, sensing, and process control [16,28,67–69]. Research progress has been reported in the field of WAAM process parameters optimization [57,60,65,70] and deposition strategy optimization [56,57,66,71–75]. Researchers have not extensively covered the review domain of optimizing WAAM processing parameters and deposition strategy in their review articles [69,76–80]. Hence, collecting and reviewing thorough data from published articles in the optimization technique and deposition strategy fields is imperative, as depicted in Fig. 3.

This article aims to review the status of recent research and development in the field of optimization techniques for the WAAM process. A comprehensive discussion is conducted on the process parameters for optimizing the WAAM process. A comprehensive analysis of several slicing and path planning strategies used in WAAM weld bead deposition is discussed. Furthermore, the optimization methods researchers employ to optimize their findings, emphasizing statistical analytic techniques, are presented. A proposed method for optimizing WAAM processes and future perspectives in process optimization are presented, followed by concluding remarks.

Table 1
Applications of WAAM technology.

Application	Welding Heat Source			
	GMAW	CMT	GTAW	PAW
Aerospace	[22–26]	[27–30]	[31–35]	[23,36,37]
Automotive	[38,39]	[40–42]	[43,44]	–
Marine	[45,46]	[47,48]	–	–
High Temperature	[49,50]	–	[51]	[52]
Corrosion Resistivity	[53–56]	[57]	[58,59]	–

2. Process parameters optimization

To fully optimize the utilization of a manufacturing process, an individual must be able to identify all the process parameters associated with that specific process. In addition, by prioritising optimization, it becomes possible to achieve both simplicity of process implementation and enhanced user experience. Hence, in order to obtain NNS components of superior quality and without any defects in the Wire Arc Additive Manufacturing (WAAM) process, a meticulous selection and implementation of a combination of process parameters such as wire

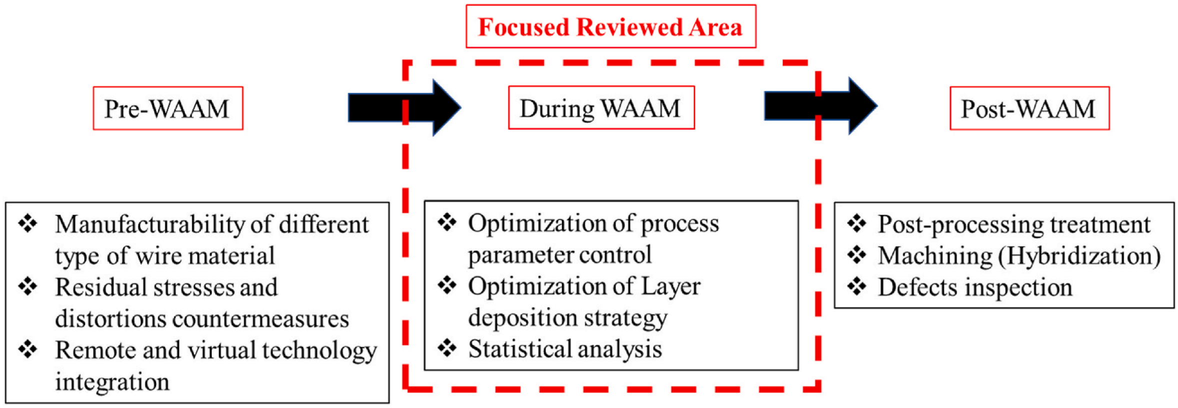

Fig. 2. WAAM difficult research hotspot.

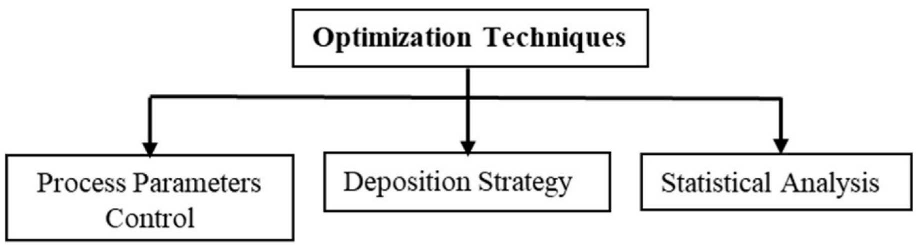

Fig. 3. Optimization technique focused research area.

diameter, wire feed rate (WFR), travel speed, welding voltage, welding current, nozzle-to-work distance (NTWD), shielding gas torch angle, and stepover distance are necessary. This section explicitly addresses the critical process parameters that significantly impact the properties of NNS components manufactured by WAAM.

2.1. Wire feed rate

The primary issue that WAAM has encountered is deciding whether to enhance the weld bead deposition rate or decrease the heat input distribution. This is because Wire Feed Rate (WFR), also referred to as wire feed speed, is closely correlate with the necessary heat input [81–84]. Hence, choosing the optimum WFR is essential to ensure that excessive slowness does not compromise the residual stress accumulated in the deposited metals. Conversely, employing rapidity might result in deformation during the formation of each layer of beads. The deposition process will generate excessive heat, leading to the remelting of previously created layers and ultimately causing microstructure and bead shape degradation. Choosing an appropriate WFR can enhance the quality of surface evenness when a low deposition rate is required. Furthermore, studies by Baffa et al. [84] have demonstrated that WFR significantly affects the appearance of ER70S-6 steel weld bead using GMAW, as shown in Fig. 4. Various WFR variations result in high-quality bead dimensions.

The manipulation and control of WFR were also affected by the heat source selected. The WAAM method, which utilises the CMT technique, employs a controlled low-heat input and low WFR to provide a consistent deposition surface structure. This effectively prevents the weld pool

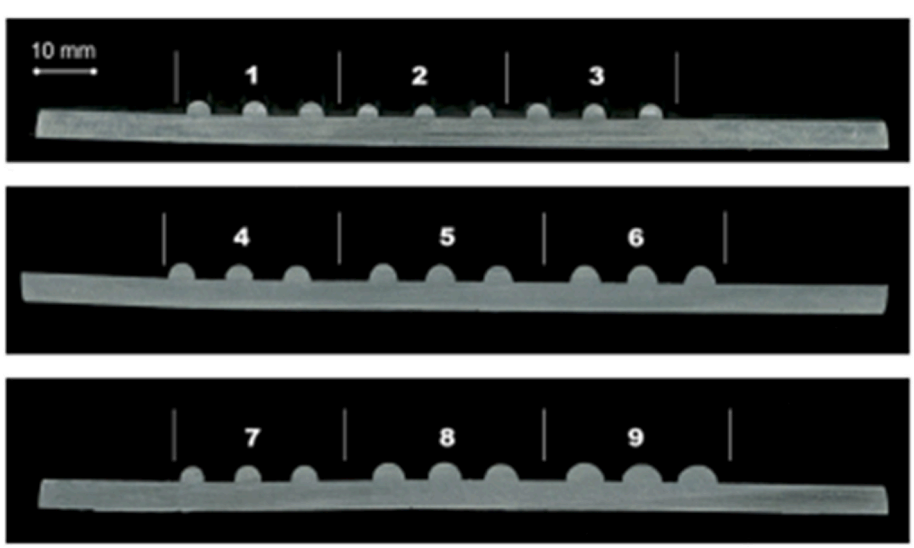

Fig. 4. Cross-sectional observation of bead dimensions using nine different WFR [60].

from overflowing or collapsing [85]. In order to get the optimal deposit quality and deposition rate, WFR is also essential [86]. In addition, increasing the WFR and energy input by giving a more significant current has been proven to be an effective method for enhancing the deposition rate [87]. The viability of the deposition technique for optimizing weld bead morphology has been established by considering WFR, welding current, travel speed (TS), substrate tilt angle, and welding torch angle [88].

Xiong et al. [89] discovered that the inclination angle of H08Mn2Si steel components is inversely proportional to the WFR values used, demonstrating the importance of WFR manipulation in optimizing the heat input supplied through GMAW. In addition, the extent of design geometry complexity for overhang features, circular patterns, and angular structures of UTP 759 Ni–Cr–Mo alloy was optimally controlled by a combination of factors, including type of heat source, current, voltage, and WFR, as shown in Fig. 5 [90]. Lower WFR values were used for non-vertical material deposition to ensure appropriate heat input, promoting adequate adhesion of the material on each succeeding layer while accounting for the effects of gravity. This demonstrated the significance of the WFR variation in influencing the ideal geometric characteristics of the component manufactured by WAAM.

Furthermore, WFR also impacts the development of welding bead characteristics, including bead height (BH), bead width (BW), and contact angle (θ). The influence of wire feed speed on bead width is challenging to control, as illustrated in Fig. 6(a). Initially, the bead width deposited reaches its maximum value but subsequently begins to diminish as the wire feed value increases. Conversely, the contact angle continues to increase with the wire feed speed, as illustrated in Fig. 6(b), suggesting that inadequate wetting has a detrimental effect on the workpiece [91]. Martina et al. [92] and C. Wang et al. [87] achieved a similar conclusion in their WAAM deposition technique for Ti–6Al–4V components using PAW heat source.

2.2. Travel speed

Along with heat input and WFR, travel speed is an important process parameter that should be precisely regulated since it substantially impacts the deposit progress, deposits geometry and thermal cycles of an adequate bead shape of H08Mn2Si steel using GMAW [93]. Travel speed is critical in achieving consistent layer-by-layer deposition in the WAAM process to manufacture NNS components with enhanced mechanical characteristics and intricate geometric designs. Higher deposition rates are possible at lower travel torch speeds, leading the welding arc to impact more on the molten weld pool (bead) than on the substrate material or the subsequently produced bead. Nevertheless, as the torch travel speed increases, the thermal energy per unit length of bead deposited will initially increase but then remain constant over time. Furthermore, an excessively high torch travel speed will result in inadequate metal supply to the deposited bead, as it diminishes the heat input distributed throughout the WAAM process, thereby influencing the melt-through depth [94]. As a result, selecting the optimum torch travel speed is essential to achieving components with improved integrity throughout the WAAM process.

According to Warsi et al. [82], arc power and travel speed are the most important criteria influencing the development of ER70S-6 steel fusion zone (FZ) geometry on a A36 steel substrate using a Computer Numerical Controlled Gas Metal Arc Welding (CNC GMAW). As travel speed rises gradually, less heat is emitted per unit length, causing the FZ's cross-sectional area to decrease. Furthermore, the geometrical characteristics of continuous single-layer aluminum deposits using CMT can be optimized by employing the optimum travel speed values with varying electric power, as denoted by P5, P6 and P7 in Fig. 7, having values of 1039 W, 1470 W, and 1666 W, respectively [95].

Travel speed was varied to identify the optimal structural integrity of components manufactured by WAAM. The findings indicate that when the electric arc travel speed increased, there was a decrease in the pores' sizes and volume fractions of each specimen, as seen in Fig. 8. This is highly beneficial for researchers aiming to reduce defects especially humping phenomenon in steel and aluminum components produced using the GMAW, GTAW, and CMT heat source [96–98].

Z. Wang et al. [99] proposed an improvement technique that combines varying travel speeds and an additional return path for each layer deposition in order to maximise high strength steel component structural integrity using CMT technique, as shown in Fig. 9. When maintaining a constant travel speed value from start to finish of a WAAM process, it is possible to deposit a bead; nevertheless, a compensation approach is required to deal with the bead's geometric irregularities challenges precisely.

Travel speed variations were frequently employed to improve the mechanical characteristics of a WAAM-manufactured component. According to research conducted by Yangfan et al. [100], the ultimate tensile strength (UTS) and yield strength (YS) of Inconel 625 increased as the travel speed increased, as shown in Fig. 10. This can be attributed to the precipitate phase that formed inside Inconel 625 when using CMT, causing a modification in grain structure and a reduction in the solid solution strengthening element.

2.3. Heat input

The arc current and voltage are other essential elements in the optimization process WAAM. They are the primary process control parameters that regulate the amount of heat input provided and dispersed, hence influencing the deposition of the weld bead. It is essential to prevent irregularly deposited beads and poor surface roughness. Additionally, an excessive influx of heat can result in the re-melting of previously deposited layers, adversely affecting the microstructure,

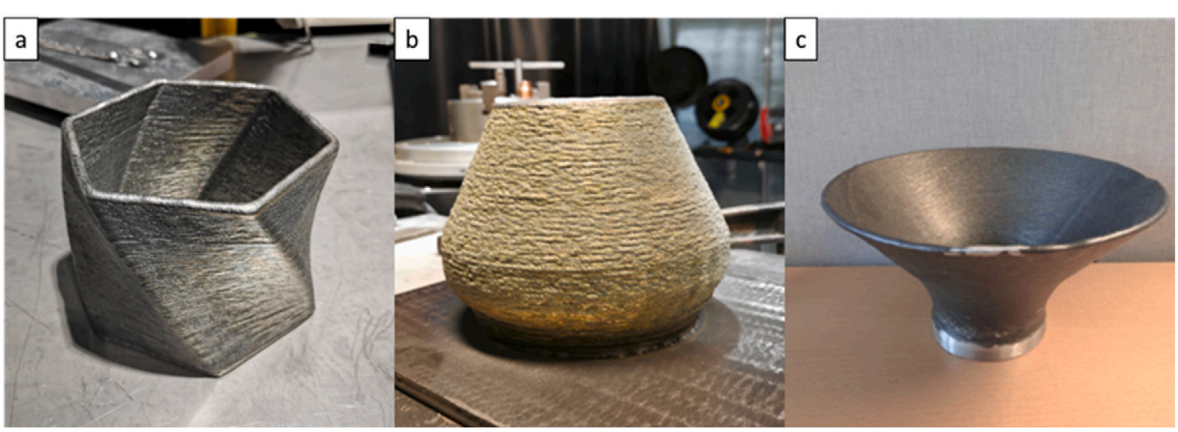

Fig. 5. The overhang WAAM structure: (a) twisting hexagon, (b) vase, and (c) bowl [90].

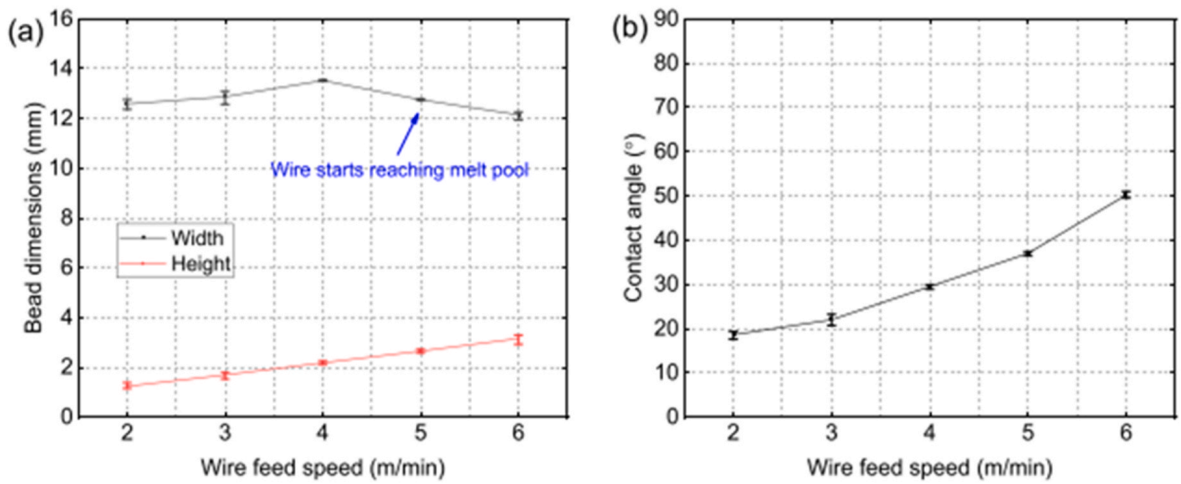

Fig. 6. The effect of wire feed speed on (a) bead dimensions, and (b) contact angle [91].

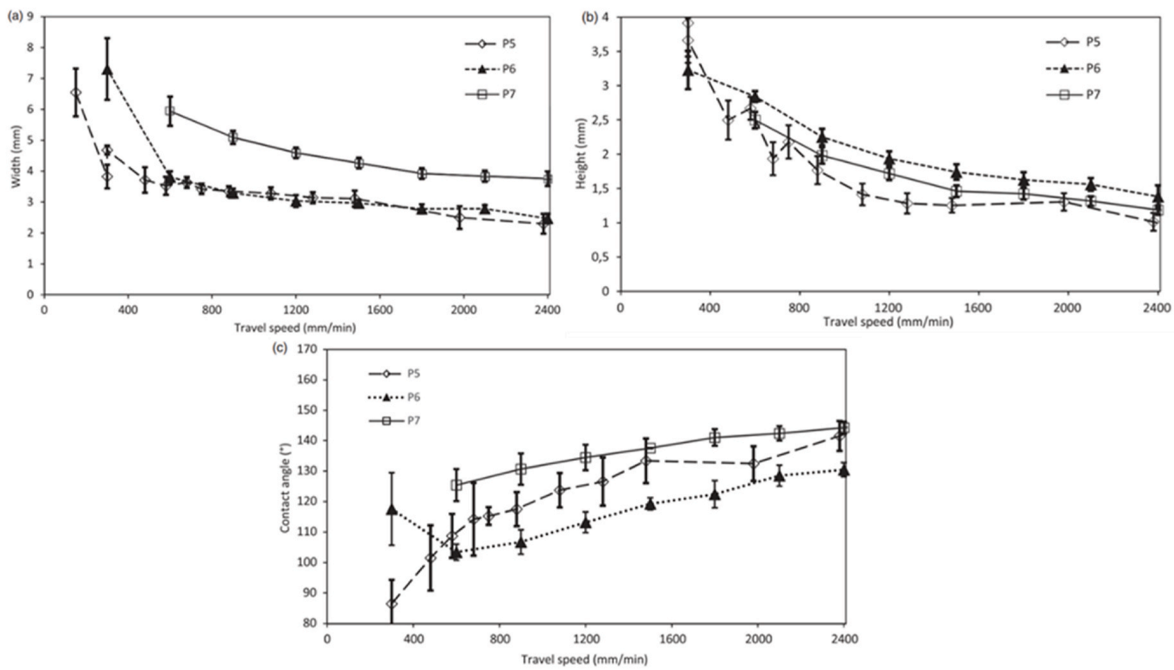

Fig. 7. Deposited bead dimensions (at varying electric power, denoted by P5, P6, P7) (a) width, (b) height, and (c) contact angle against the travel speed (mm/min) [95].

dimensions of the bead, and its mechanical characteristics. It is essential to optimize the current and voltage to enhance the overall efficiency of the process. Proper and steady regulation of heat input is critical to achieving the desired melting rate for metal deposition in WAAM [101]. The arc current, voltage, and travelling speed are the main factors that determine the appropriate thermal profile for WAAM. The heat input in the WAAM process, supplied by the heat source (GMAW, CMT, GTAW, PAW), refers to the amount of heat required to enable the deposition of metal on a substrate surface. This heat distribution is necessary to establish the required thermal gradient and ensure a proper heat cycle from melting to cooling to solidifying the deposition. The heat input is typically measured in joules per mm and derived from the subsequent equation (1) [102]:

$$Q = \frac{V\ (U) \times I\ (A)}{TS\ \left(\frac{mm}{min}\right)} \tag{1}$$

Where Q represents the heat input, V is voltage, I represents current, and TS is the travel speed of the torch.

$$Q = \eta\ \frac{V\ (U) \times I\ (A)}{TS\ \left(\frac{mm}{min}\right)} \tag{2}$$

The heat input calculation in the WAAM process has been modified by including the thermal efficiency coefficient (η) in equation (1). The value of η is influenced by the arrangement of the heat source in the WAAM process, the design of the deposition geometry, and the type of material used, as depicted in equation (2) [103–105]. This allows for the optimal amount of heat required to melt down the metals in the WAAM process. Thereby minimising defetcs such as undulated surface morphologies, inconsistent layer deposits, and time required for post-processing treatment.

Controlling interpass temperature and adhering to heat input standards are among effective methods for maintaining thermal boundary

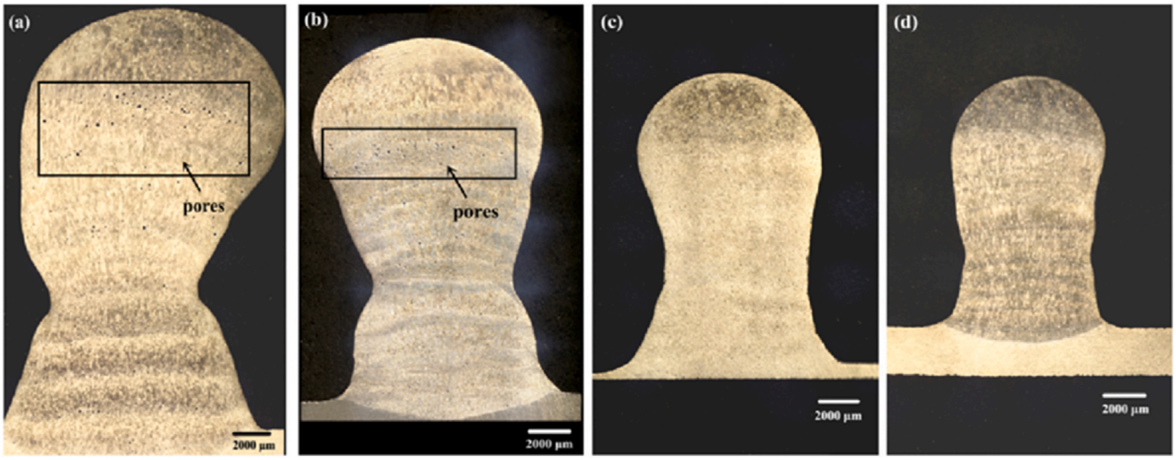

Fig. 8. Deposited metal's cross-sectional observation at various travel speed values: (a) 150 mm/min, (b) 250 mm/min, (c) 350 mm/min, and (d) 450 mm/min [96].

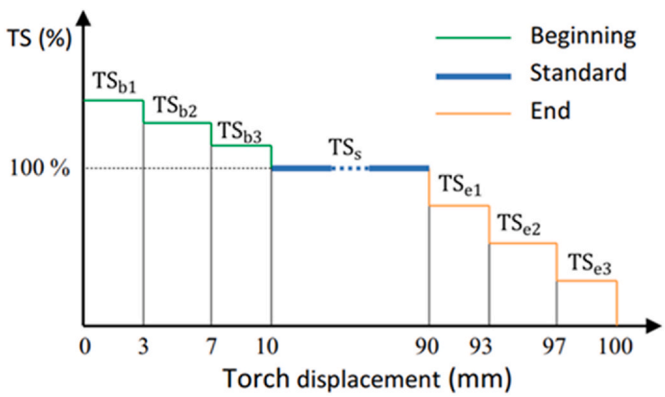

Fig. 9. Illustration of different travel speed configurations [99].

stability in WAAM process. Hence, interpass optimization seeks to minimise the temperature gradient at the fusion line between two layers. Meanwhile, it is essential to control heat input to eliminate the adverse effects of thermal disturbance resulting from heat accumulation [106]. There are numerous significant factors that have influenced the optimization of heat input in the WAAM process. Table 2 displays the correlation matrix among the factors that influence the optimization of heat input with regard to the performance of the manufactured WAAM product. The factor's influence on the performance of the WAAM product is designated as STRONG (S) if it is highly significant. At the same time, it is classified as WEAK (W) if it still has an impact but is not as significant. Based on the matrix table, the heat input, controlled by voltage and current, has the most significant impact on the overall performance of a WAAM product. Meanwhile, the structural integrity, which is determined by the Effective Wall Thickness (EWT) and Surface Waviness (SW), is greatly affected by each component that influences the optimum heat supplied.

According to Lervåg et al. [150], various material characteristics can be linked to the accomplishment of an optimized WAAM process through variation of heat input. These characteristics include tensile data, hardness value (HV), toughness, fracture morphology, microstructure characterisation, and the formation of intermetallic compounds. In addition, variations in heat input will substantially impact the distribution of optimum pore content and the sensitivity of the deposition process to hydrogen absorption [104]. Increased heat input and the use of various heat source modalities considerably contribute to the high abundance of pore numbers [151].

Furthermore, by utilising varying current (A) values, the %EP time cycle for each aluminum layer deposited can be optimized, leading to an optimal outcome since the cooling mechanisms operate linearly with GTAW heat input [152]. Controlling the quantity of heat input supplied is an additional method for optimizing the WAAM process, given that the phases of microstructure obtained are substantially correlated with the thermal cycles of each layer [153]. Additionally, weld bead geometry can be optimized by modulating the heat source of the WAAM process in order to improve control over process parameters. In their study, Greebmalai et al. [154] found that using double pulse current (DP-GMAW) for optimal heat input instead of single pulsed current

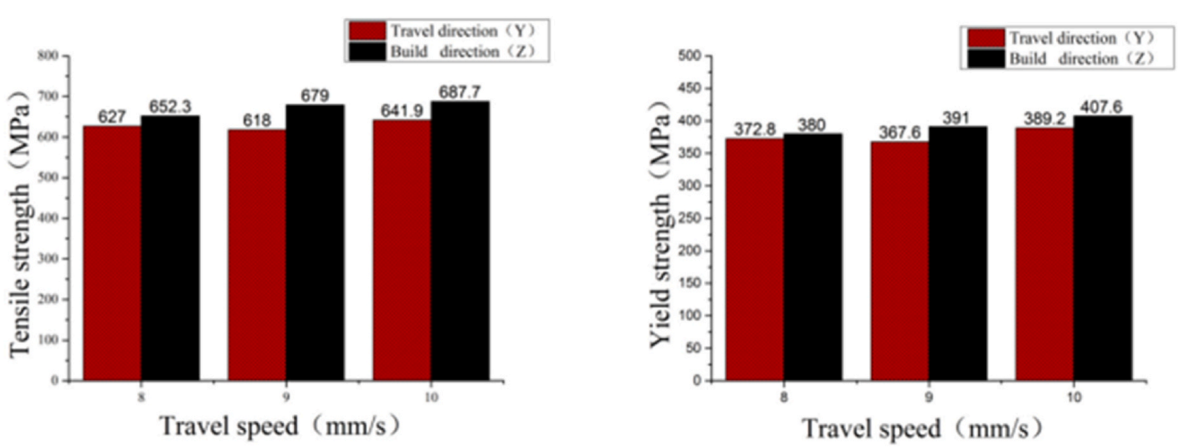

Fig. 10. (a) Ultimate tensile strength and (b) yield strength of the travel and build direction at various travel speeds [100].

Table 2
Relationship matrix between factors affecting the optimization of heat input with the finished product performance.[22,55–57,60,63,65,66,70,96–98,107–149]

(S = STRONG, W = WEAK, N = NO EFFECT)

Factors \ Performance	Structural Integrity	Surface Finish	Substrate warping	Residual Stress	Porosity	Cracks	Hump	Tensile Strength	Hardness	Micro-structure
Type of heat source	**S [107-110]**	**W [108]**	**N**	**N**	**S [66, 111-113]**	**N**	**S [97, 98]**	**N**	**W [114]**	**W [107]**
Type of wire material	**S [115]**	**S [116]**	**S [117]**	**W [118, 119]**	**S [66, 113, 120, 121]**	**S [66, 113, 122]**	**N**	**S [55, 123-129]**	**S [127, 130, 131]**	**S [56, 124, 127, 129, 132, 133]**
Wire Feed Speed	**S [57, 134]**	**S [57, 135]**	**N**	**S [65]**	**S [136]**	**S [57]**	**W [137]**	**S [60, 65]**	**S [60, 65]**	**S [57, 138]**
Travel Speed	**S [57, 137]**	**S [70, 135, 139]**	**N**	**N**	**W [140, 141]**	**S [70]**	**S [137, 142]**	**S [60, 65, 96, 139]**	**S [60, 65, 96, 139]**	**S [57, 96, 138, 139]**
Voltage (V)	**S [70, 143]**	**S [70]**	**S [144]**	**S [145, 146]**	**S [147]**	**S [70]**	**N**	**S [70]**	**S [70]**	**S [65, 147]**
Current (A)	**S [70, 105, 143, 148]**	**S [70, 135]**	**S [144]**	**S [145, 146]**	**S [147]**	**S [70]**	**S [22, 149]**	**S [70]**	**S [70]**	**S [65, 147]**

resulted in notable benefits in terms of the appearance of a single bead when using ER5356 aluminium alloy wire. Heat input can be optimized by using a by-pass current to improve deposition efficiency in an additive manufacturing (AM) system [155].

2.4. Shielding gas employed

Another crucial factor that needs careful consideration for optimization of WAAM process is the selection of shielding gas. This is due to the challenges associated with shielding gas employed and its influence on performance of the finished WAAM product. The welding torch setup provides the shielding gas in the majority of circumstances. Table 3 displays the correlation matrix between the factors that influence the optimization of shielding gas and the ultimate performance of the WAAM product, as reported in various studies. Based on Matrix Tables 3 and it is evident that fewer variables influence the end product's performance compared to Matrix Table 2.

However, the use of shield gas still significantly influences some characteristics, such as the structural integrity and mechanical behaviour of the WAAM-manufactured product. This is crucial for enhancing the characteristics of the product. Furthermore, an inadequate flow rate of shielding gas can have a detrimental impact on the structural integrity for any type of material regardless of any type of heat source employed. This can lead to the formation of voids and porosity owing to chemical reactions with ambient gases [173]. In order to prevent the formation of defects during bead deposition, it is necessary to ensure that an adequate amount of shielding gas is supplied within the WAAM system. This gas acts as a barrier to protect the surrounding area of the weld pool and prevents chemical reactions with atmospheric gases. Doing so effectively prevents the formation of harmful oxides and nitrides [174]. Many researchers have recently implemented innovative methods to optimize shielding gas conditions to emphasise improved deposited material characteristics in WAAM. These methods include using inert chambers or flexible tent shielding to manage turbulence problems, improve surface finish, and improve deposition efficiency (DE) [158, 164].

The optimal composition ratio of the shielding gas used in the WAAM process is critical because it affects the heat transfer mechanism during bead deposition [167]. Moreover, it effectively inhibits the occurrence of arc wandering phenomena in extremely reactive substances, such as

Table 3
Relationship matrix between factors affecting the optimization of shielding gas with the final product performance.[103,134,140,142,156–172]

= STRONG, W = WEAK, N = NO EFFECT)

Factors \ Performance	Structural Integrity	Surface Finish	Substrate Warping	Residual Stress	Porosity	Cracks	Hump	Tensile Strength	Hardness	Micro-structure
Type of gas	**S [103], [156], [157]**	**S [158]**	**N**	**N**	**S [159], [160]**	**N**	**N**	**S [161]**	**S [162]**	**S [163]**
Gas flow rate	**S [164], [134]**	**S [164]**	**N**	**N**	**S [159], [142]**	**N**	**N**	**W [165], [134]**	**W [165], [134]**	**N**
Gas composition (ratios and purities)	**S [166], [167]**	**S [168]**	**N**	**N**	**S [162], [140]**	**N**	**N**	**S [169], [168], [170]**	**S [171], [166], [165]**	**S [172], [166]**

titanium and aluminium alloy. Da Silva et al. [175] investigate the effect of varied oxide compositions in argon-based shielding gases of thin aluminum wall structure using GMAW, which successfully optimises the WAAM process by minimising defects formed. Green et al. [170] enhanced the performance of GMAW-WAAM by adjusting the composition ratio of shielding gas for the layer deposition of Grade 91 steel. This allowed them to control the precipitation process and carbonitride morphologies in enhancing mechanical properties of Grade 91 steel at high temperature. In their study, Yamaguchi et al. [103] investigated the issues associated with the metal transfer behaviour of mild steel using GMAW after being subjected to various type of shielding gases. Fig. 11 illustrates the fluctuations in current and voltage seen during the application of 1.17 kJ/cm of heat input for the deposition of five successive layers. The experiment was conducted using Ar gas in case (a) and CO_2 gas in case (b). It has been demonstrated that the type of shielding gases has a substantial impact on the optimization of the WAAM process. N_2 and Ar shielding gases have different impacts on bead formation due to variances in physical and chemical characteristics [163]. The quality of WAAM components can be significantly influenced by the appropriate adjustment of the composition of shielding gases, which in turn affects microstructure characterisation and fracture morphology [162].

2.5. Wire selection

The selection of wire material and its diameter is an important consideration that greatly influences the structural integrity and product quality of NNS WAAM components. The diameter of the wire has a significant impact on the distribution of heat input, deposition rate, and overall quality of the deposited bead. Therefore, controlling the width of the molten pool (WMP) is successfully achieved by optimizing the wire diameter [176]. Varying the wire diameter has a considerable impact on both the breadth and height of the bead [137].

Additionally, implementing numerous wire-feeding mechanisms can enhance material characteristics and control the formation of essential grain structure, grain refining process, and phase transitions [33,177,178]. Thus far, incorporating multiple wire feeding systems has shown to be a very effective and practical solution for addressing material composition issues associated with manufacturing complex geometric components in WAAM [179]. Studies by Feng et al. [180] suggest that the stainless-steel deposition rate of a double-wire feed plasma arc WAAM system may also be improved. Additionally, a more refined microstructure may be produced by employing a dual wire feeding method to enhance the mechanical properties. The presence of two wires results in a notable enhancement in mechanical properties while reducing the number of pores for aluminum alloys using CMT [181,182]. The wire feeding system may be pre-heated to enhance the grain structure, resulting in superior hardness quality [183,184].

Qi et al. [185] developed a dual Wire WAAM system using GTAW to improve the materials characteristics by altering the WFR based on the usage of different types of aluminum wires for layer deposition. Fan et al. [186] developed and verified the feasibility of similar research. Additionally, Somashekara et al. [187] successfully executed a GMAW-based twin-wire weld deposition process using ER70S-6 and ER110S-G filler wires. The mechanical properties, particularly the hardness values, have been effectively enhanced.

Additionally, the selection of wire quality is critical, as any imperfections or defects in the wire will have a consequential impact on the solidification of the deposited beads, thereby influencing the overall strength of the manufactured component. Variation wire size or the presence of cracks and scratches on the wire surface can result in the formation of voids and porosity, which in turn leads to the propagation of cracks inside the deposited bead and layer [188]. By employing high-quality wires, which Murav'ev et al. [189] defined as wires without any surface fractures or scratches, effectively decreases the porosity of the solidified weld pool in molten titanium alloy.

Based on the study conducted in section 2, it can be concluded that the Wire Feed Rate (WFR), Travel Speed (TS), heat input, type of shielding gas, and gas flow rate are the primary process factors in the WAAM technique that have a major impact on the structural integrity of a WAAM structure. A correlation between frequently utilised welding wire materials and specific sets of optimized parameters for the Wire Arc Additive Manufacturing (WAAM) process can be established. In section 5, a radar chart is proposed and developed based on the current trend and research progress in WAAM. The next section will focus on the various deposition strategies utilised in fabricating Wire Arc Additive Manufacturing (WAAM) components. Various methodologies were employed to achieve optimum manufacturing components with superior and excellent structural integrity.

3. Optimization strategy for layer deposition

3.1. Deposition strategy

An essential characteristic of WAAM technology is the ability to achieve a minimal buy-to-fly (BTF) ratio, defined as the mass ratio of the raw materials used to fabricate a component to the final component. BTF for a sliced layer can be calculated by equation (3) [190]:

$$BTF = \frac{A_{deposited}}{A_{desired}} \tag{3}$$

"$A_{desired}$" refers to the desired area of the shape determined by the sliced CAD model design. On the other hand, "$A_{deposited}$" indicates the actual area that is deposited, which is greatly influenced by the path

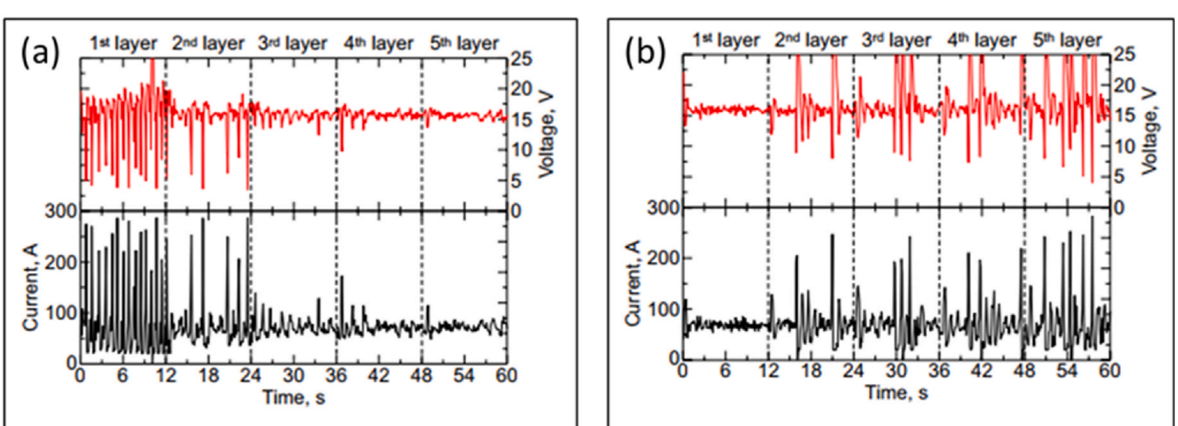

Fig. 11. Variations in current and voltage under different shielding gasses, (a) Ar and (b) CO_2 [103].

planning strategy used. In contemporary industry, a low buy-to-fly ratio is favoured for its ability to streamline the machining process while minimising costs. In order to effectively incorporate such characteristics, it is essential to design an efficient deposition strategy and employ an optimal technique. As illustrated in Fig. 12, deposition strategy is typically divided into the following order: 3D CAD model layer slicing path, the tool-path selection process, and path planning algorithm sequences.

Due to its dynamic nature, the WAAM process faces various challenges and issues during bead deposition. These include varying metal transfer behaviour and heat source use, such as direct crossing, which leads to peaks in thin wall structures. Other challenges include the remelting of previously deposited beads or layers, inaccurate path patterns for opposite angles, and the deformation of beads deposited on overhanging structures. These factors significantly impede the efficiency of the process. As a result, an optimization technique is necessary to accommodate the various deposition strategies implemented [28,66]. Nowadays, much research is being conducted on WAAM in an effort to resolve these issues through the implementation of innovative techniques and methods for path planning, segmentation algorithms, and tool path generation. Three commonly employed deposition strategies for layer-by-layer bead deposition include oscillation, parallel, and weaving, as seen in Fig. 13 [191].

By incorporating multi-axis movement capabilities into additive manufacturing (AM), the process WAAM has become capable of fabricating components without the use of support structures. In order to optimize this capability, a robust and automated algorithm for slicing 3D CAD models in multiple directions has been developed. This algorithm, which includes the Silhouette edges projection algorithm [192], the Transition wall algorithm [193], and the Centroid axis extraction technique [194], efficiently divides the models into layers with minimal need for supportRecently, multi-directional WAAM techniques have been implemented to fabricate complex geometry components with overhang characteristics. This approach is advantageous for industrial applications, allowing for high productivity while minimising capital expenses. The complexity of building an automated system for industrial applications increased due to the interdependence of deposition sequencing and single-layer path planning, making the optimization of the WAAM path planning process more challenging. An essential aspect of the WAAM process is the creation of a path-planning algorithm. This algorithm directs the movement of the deposition tool (weld head) to fill the 2D layers that depict the cross-sectional geometry of the components [195]. Moreover, this algorithm allows for the integration of streamlined work ethics to enhance future process enhancement.

3.2. Tool-path pattern

In order to enhance the diffusion mechanisms of WAAM, it is imperative to incorporate appropriate tools and deposition strategies during the process planning phase [142]. The toolpath must adhere to the geometric characteristics and dimensions of the specified structure while also being consistent with the implemented WAAM methods. Various tool-path patterns have been developed for the implementation of deposition strategies in general for WAAM procedures, as indicated in Table 4. WAAM technology incorporates a multi-directional processing system that can move in the ±X, ±Y, and ±Z directions. Consequently, the configuration of the WAAM system necessitates a distinctive trajectory pattern that allows the automated system to travel in the (X, Y, Z) directions [196].

3.3. Research progress on WAAM deposition strategy

Table 5 presents a summary of available research efforts focused on deposition strategies that have a substantial influence on enhancing the characteristics of final components produced by WAAM. Researchers can utilise specific deposition strategies outlined in Table 5 to enhance the existing characteristics of WAAM structures.

In summary, the substantial detail presented in this section highlights that the deposition strategy significantly impacts the factors that influence the fabrication of WAAM components. Data and findings from various literature sources support this conclusion, demonstrating that slicing and path-planning algorithms are essential components in optimizing the deposition strategy. A significant amount of effort and concepts were effectively implemented in optimizing strategies to address a wide range of issues, allowing for the optimal integration of WAAM results into deposition strategies or the development of path-planning algorithms.

4. Statistical optimization techniques

The optimization and analytical measurement of process parameters in multi-variable WAAM technology are intricate and multifaceted. This complexity arises from the influence of various factors and design challenges on the mechanics of the process. Therefore, achieving an optimal condition necessitates a deep understanding of manipulating multiple combinations of process parameters. Thus, it has become common practice in various manufacturing industry over the last several decades to adopt effective techniques or methodologies, such as statistical analytic calculations, to facilitate this transformational shift [241–245]. Employing such strategies can yield several benefits and contribute to the transformation of Industrial Revolution (IR) 5.0, leading to scientific progress. Statistical analysis is an efficient and successful tool for reducing lead time and capital costs in AM industries. This is because it allows for systematic pre-planning of trial-and-error methods. However, the global investigation of optimizing multi-variable process parameters for high deposition rates about thermo-mechanical and metallurgical characteristics still in progress and continue to developed. As a result, a vast amount of information with varying results has been reported that will be highlighted in this section concisely.

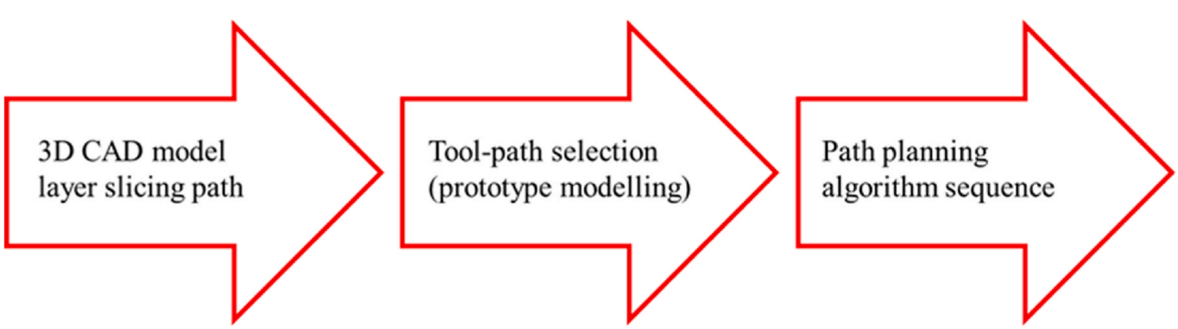

Fig. 12. Process flow in deposition sequence for typical WAAM process.

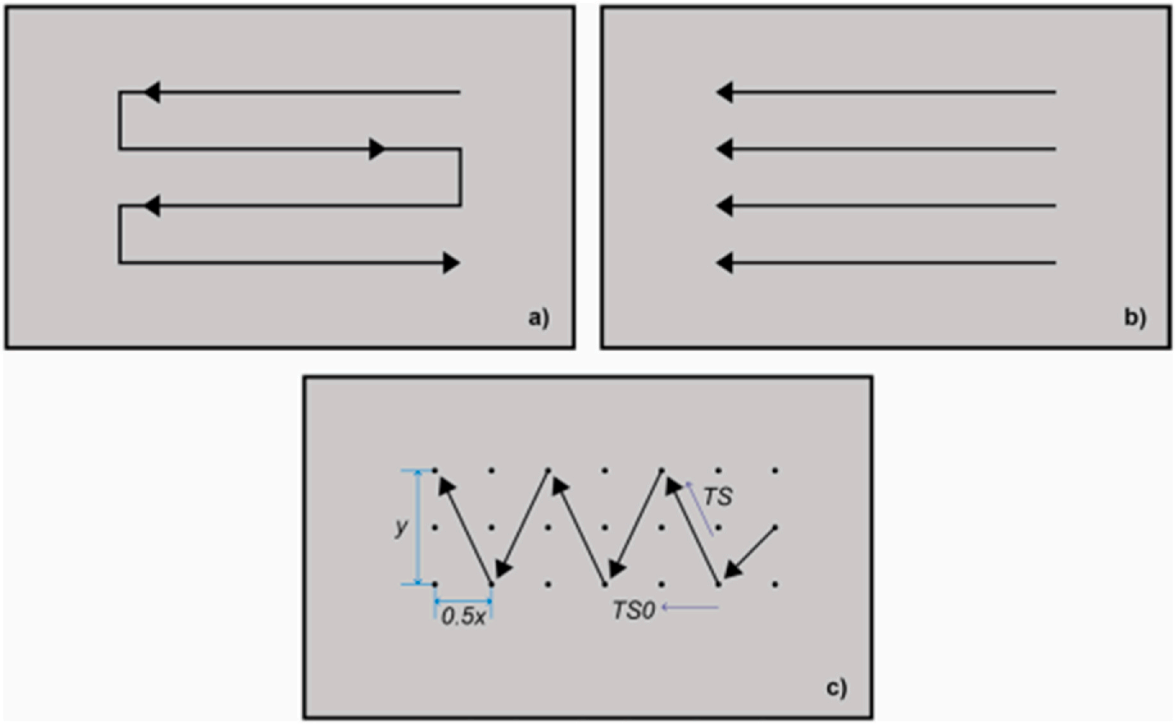

Fig. 13. Deposition strategies: (a) Oscillation, (b) Parallel, (c) Weaving [191].

4.1. Application of statistical tools in WAAM

Researchers have developed and put into practice a variety of evaluation and assessment techniques to evaluate the contribution of process parameters and optimize the WAAM process, as outlined in this section [246]. The research methods utilised in this study consist of Design of Experiments (DoE) techniques, including the Taguchi method and the Full Factorial technique [247], p-values from Analysis of Variance (ANOVA) [248], and regression modelling [249,250]. These techniques were recognised as crucial tools in facilitating the analysis required for process optimization and quality enhancement.

In order to gain a greater understanding of and effectively control the critical challenges of the WAAM process, such as residual stress and deformation, Dinovitzer et al. [10] conducted a set of experiments utilising the L_{16} (4^4) orthogonal array (OA) Taguchi method and one-way ANOVA. The objective was to ascertain the correlation between each factor and response when optimizing material characteristics. This was achieved by manipulating four distinct factors: wire feed rate (mm/min), travel speed (mm/min), current (A), and argon flow rate (CFH). The response obtained showed a notable contribution, indicating that the depth of melt melt-through and surface roughness do not interact with wire feed speed. However, there is a linear rise in bead height.

The process optimization approach is essential for identifying the future potential of WAAM applications. The exceptional focus on height variation as the determining factor poses a challenge in manufacturing WAAM components with consistent structural integrity. Rosli et al. [251] examine the correlation between process parameters and the variation in weld bead height in GMAW-based WAAM wall structures. For this purpose, they employ the Taguchi design with signal-to-noise (S/N) ratio analysis. Likewise, Zavdoveev et al. [252] employed a comparable strategy to develop an efficient welding mode for the pulsed GMAW-based WAAM process. They aimed to increase the deposition rate while maintaining cost-effectiveness. This study presented a method for optimizing the WAAM process by utilising L_9 (3^4) orthogonal arrays (OAs) Taguchi method, and S/N (signal-to-noise) ratio analysis. The objective was to determine the minimum number of experiments required to investigate the impact of each process parameter on the overall WAAM process. As a result of the optimization process, the hardness values increased, leading to greater strength. Additionally, the observed grain structure had undergone improved grain refining.

In their study, Kumar et al. [253] described using a genetic algorithm (GA) to optimize the selection of process parameters for producing NNS components with the dual objectives of minimising void and material waste. GA is an alternative optimization analysis instrument that operates on the principles of stochastic search engine mechanics [254]. In order to forecast the geometry of beads deposited via the WAAM process, models based on response surface methodology (RSM) are constructed using experimental data collected via the Box-Behnken Design (BBD) [255]. The optimization of bead geometry was conducted utilising the response optimizer utility in MINITAB 17 software in conjunction with the desirability function approach. It is possible to fabricate a component with minimal cavity formation and optimum material yield by utilising the optimized process parameters.

Controlling surface morphology and metallurgical behaviour is quite challenging when employing WAAM technology to deposit metals for industrial purposes. Mai et al. [70] examine the optimization of process parameters for thin-walled structures made of 308L stainless steel. They specifically investigate the impact of process stability on mechanical properties and microstructure features. The response of the process parameters used in the experiments resulted in the prediction of the bead geometries, which include the width and height of the beads. The prediction models were developed using RSM and ANOVA. These models were represented by a second-order regression equation. The experimental plan was established using the BBD (Box-Behnken Design) approach. TS has been discovered to have distinct impacts on the shapes of the beads generated. Specifically, the beads' width increases linearly as the applied voltage increases, while the effects on the height of the beads are different. The determined optimal process parameters for solving the multi-objective optimization problems are as follows: current, I = 122 A, voltage, U = 20 V, and TS = 368 mm/min. A. Singh et al. [134] employed a similar method to optimize the factors that impact the width and height of beads in a thick wall structure produced from SS410 wire. These variables include WFR, TS, and gas flow rate. The optimized

Table 4
Summary of WAAM tool-path pattern.

Tool-path pattern	Illustration	References
Raster		[197,198]
Zigzag		[199–201]
Contour		[202–204]
Spiral		[118,205–207]
Continuous		[208–210]
Hybrid	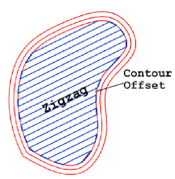	[71,74, 211–214]
Medial Axis Transformation (MAT)	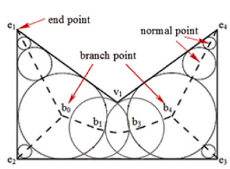	[190,215–218]

parameters are WFR = 5.5 m/min, TS = 63 cm/min, and gas flow rate = 13 liters/min. The WAAM component manufactured does not exhibit any solidification cracking or lack of diffusivity.

In order to optimize the geometry of the weld bead for GMAW-based WAAM of 2.25 Cr-1.0 Mo Steel, a comparable approach was utilised by Vora et al. [256]. The BBD technique and ANOVA were used to conduct experiments and examine the collective effects of numerous process factors, including WFR, TS, and voltage. In addition, the response parameters were further optimized by successfully using the Teaching-Learning-Based Optimization (TLBO) method [257]. In addition, Rosli et al. [258] optimized the process parameters of micro PAW, which include wire feed speed, travel speed, and pulse. Similarly, Banerjee et al. [259] optimized the process parameters of GMAW, which include wire feed speed and travel speed, using the same approaches. Gufran et al. [260] employed a distinct technique to examine the behaviour and characteristics of the weld bead geometry in the GMAW-based WAAM process for low-carbon steel. In order to simplify process planning, they selected the two most important process parameters, current and travel speed, to study the impact of deposition ratio (DR) on the weld bead. They used response surface methodology (RSM) and analysis of variance (ANOVA) to investigate this effect. Regression equations of the second order were effectively formulated and employed to design prediction models for bead geometries. Subsequently, ANOVA is utilised to assess the adequacy of the prediction models.

The process of metal droplet transfer in WAAM technologies is

Table 5
Deposition strategy employed in WAAM (W = Welding Wire, S = Substrate).

Year	Reference	Welding source	Material System	Deposition Strategy
2003	[71]	GMAW	W = 0.8 mm ER70S-6 S=SS308	Higher heat input supplied at the start and gradually reduced until the end of deposition to achieve the intended density and height structure.
2011	[72]	GMAW	W = 1.2 mm H08Mn2Si S = 10 mm S235JR	Use two different deposition directions, (1) same direction and (2) reverse direction where layer deposition in the same direction proved to be better than the reverse deposition sequence.
2012	[73]	CMT	1. W = 0.8 mm ER70S-6 S = 15 mm S355 2. W = 1.2 mm ER4043 S = 12 mm AA6082	Propose an oscillation deposition strategy for inclined wall with angles of 15°, 30°, 45°, and 60° which successfully overcome hump formation.
2014	[74]	GMAW	W = 1.2 mm ER70S-6	The use of a continuous tool-path generation technique, which combines zigzag and contour pattern deposition strategies, results in the formation of a convex polygon structure and leads to enhanced surface accuracy.
2015	[75]	GMAW	W = 1.2 mm ER70S-6	Use two phase Medial Axis Transformation (MAT): phase 1, MAT geometry preparation; and phase 2, path generated from medial axis which improved structure quality and material efficiency.
2015	[219]	GMAW	W = 1.2 mm ER70S-6	Proposed Tangent Overlapping Model (TOM) as a countermeasure to achieve higher multiple bead geometry accuracy whilst reducing material waste optimally.
2016	[220]	GMAW	W = 0.8 mm ER70S-6 S = 12 mm S235JR	Six different deposition strategies have been developed to optimize components with T-crossing features by maintaining height precision for each layer while reducing porosity and residual stress.
2016	[215]	GMAW	W = 1.2 mm ER70S-6	Develop an adaptive Medial Axis Transformation (MAT) path planning algorithm using single bead Artificial Neural Network (ANN) model and multi-bead geometry model base on Tangent Overlapping Model (TOM) to produce void free bead deposition.

(continued on next page)

Table 5 (*continued*)

Year	Reference	Welding source	Material System	Deposition Strategy
2016	[221]	GMAW	W = 1.2 mm ER70S-6	Employ Medial Axis Transformation (MAT) path planning algorithm alongside Taguchi method to automate the fabrication of complex geometries.
2017	[222]	GMAW	W = 0.6 mm ER70S-6	Utilise an open-source software, *CuraEngine* to enable the integration of automated slicing of a 3D model to improve slicing function by enhancing bead resolution widths.
2018	[223]	CMT	W = ER4043	Propose a slicing algorithm consist of heuristic method capable of solving complex symmetrical structural features problems.
2018	[224]	GMAW	W = 1.2 mm ER70S-6 S = 10 mm Mild steel	Two distinct path patterns were used to construct an upright rectangular wall structure. The first approach involved welding in a zig pattern with a unidirectional welding direction, while the second way involved welding in a zigzag pattern with alternating welding directions. It was found that the zigzag method had better characteristics compared to the zig method.
2019	[116]	CMT	W = 1.2 mm MARVAL 18S (maraging steel)	Employ oscillation, parallel, and weaving strategies to fabricate 10-layer wall structure with 120 s interlayer cooling time between each deposition in which weaving strategy led to excellent surface finish.
2019	[225]	GMAW	W = 1.2 mm ER4043	Employ three distinct optimization strategies: (1) deposition by weaving, (2) precise control of arc ignition and extinguishing, and (3) localised measurement combined with milling method to minimise variations in layer heights.
2019	[153]	GMAW	W = DSS ER2209 S = 27 mm DSS 2205	Employ two type of deposition strategy: Alternate direction and one direction deposition path to achieve layers with uniform height.
2020	[226]	GMAW	W = 1.2 mm ER70S-6 S = 8 mm S235JR	Employ two deposition techniques: oscillatory and overlapping strategies to fabricate complex geometries, crossing's structure, curvature, and variety of wall thickness.
2020	[227]	GMAW	W = 1.2 mm ER70S-6 S = 8 mm S235JR	Employ control volume concept by comparing between two different deposition strategy: oscillatory and overlapping strategies to minimise defects.
2020	[60]	CMT	W = 1.2 mm ER120S-G S = 10 mm S355	Employ oscillation and parallel deposition strategies to produce single bead welds and wall geometries which reveal lower yield strength is achievable.
2020	[228]	CMT	W = 1.2 mm SS316L S = 15 mm SS316L	Employ weaving strategy whilst increasing the torch angle yield excellent surface morphology alongside grain refinement.
2021	[229]	CMT	W = 1.2 mm ER2319 S = 12.7 mm AA6082-T6	Utilise oscillation and parallel deposition techniques to construct a thicker segment of a linear wall in order to enhance its hardness.
2022	[191]	CMT	W = 1.2 mm ER70S-6 S = 20 mm Carbon steel plate	Perform oscillation, parallel, and weaving strategies to fabricate walls, blocks, and bimetal structure.
2022	[57]	CMT	W = 1.6 mm DSS ER2209 S = 10 mm Q235A steel	Two additive paths were used to deposit 10-layer wall structure, unidirectional and reciprocating addition.
2022	[230]	GMAW	W = 1.2 mm ER70S-6 S=S235JR	Three distinct deposition strategies were utilised to build a wall structure with an inclined angle, specifically for a particular component dimension. Three different strategies are being tested: (1) the go strategy, (2) the go strategy with changed entrance and exit conditions, and (3) the back-and-forth method.
2022	[56]	GMAW	W = 1.2 mm FCWA-AM Super Duplex Stainless Steel (SDSS)	Different process parameter were applied for each nth layer to achieve austenite ratio of 45%.
2022	[131]	GMAW & PAW	W = 1.2 mm ER70S-6 and ASS 316L S = 10 mm ASS 316L	Use two different deposition techniques: superimposed and overlapped strategy to deposit defects-free bimetallic wall structure.
2022	[231]	GTAW	W = 1.0 mm ASS 316L (ER 316LSi) and Inconel 625 (ER NiCrMo-3) S = 6 mm Mild steel plate	FGMs properties were compared by employing two different deposition strategies: direct interface and smooth transition where direct interface has proven to be a superior strategy in terms of strength and elongations upon failure.

(*continued on next page*)

Table 5 (*continued*)

Year	Reference	Welding source	Material System	Deposition Strategy
2022	[232]	CMT	W = 1.2 mm Ti–6Al–4V S = 4 mm Ti–6Al–4V	Employ zigzag deposition strategy on different condition of CMT transfer modes to achieve stable structure properties.
2022	[233]	PAAM	W = 1.2 mm Ti–6Al–4V S = 4 mm Ti–6Al–4V	Compare two sets of PAAM specimen: (1) layer deposition without rolling force, (2) layer deposition with in-situ rolling force of 15 kN.
2022	[234]	CMT	W = 0.9 mm ER70S-6 S = 10 mm Q235 steel plate	Suggest an innovative approach for automating the path planning process in robotics by including an Automated Robot Offline Programming (AOLP) engine. This approach uses a collision matrix as a heuristic strategy to simplify the complexity of the path-planning process.
2022	[235]	CMT	W = Kiswel 1.2 mm M-308 S = 25 mm SS304	Integrating a regression model with a Support Vector Machine (SVM) classifier can diminish the variation in bead deposition between the arc strike zone and the intermediate zone.
2022	[236]	CMT	W = 1.2 mm ER4043 S = 3.15 mm AA6061-T6	Employ two different path planning strategy, (1) Uni-directional, and (2) Bi-directional in reducing heat input.
2022	[237]	CMT	W = 1.2 mm Aluminum ER2319 S = 10 mm AA6082-T6	Utilise two deposition techniques for torch movement, namely the Hatching strategy and the Circling method, while alternating the travel direction from odd to even layers to ensure stability.
2022	[238]	PAW	W = 1.2 mm ASS 316L-Si S = 15 mm S235JR	Optimal high-quality X-Cross intersection geometry's structure were obtained through the employment of both Cross-waving and Cross-Overlapping deposition strategies.
2023	[239]	CMT	W = 1.2 mm Low alloy steel (Fe–2Mn–1Si-0.08C) S = 10 mm Low carbon steel (Fe-1.4Mn-0.35Si-0.2C)	Multi-pass paths with varying center distances and extra gap-fill paths have been employed through the utilization of Artificial Neural Network (ANN) to produce gap-free components.
2023	[240]	CMT	W = 1.2 mm Aluminum ER2319 S = 10 mm 2Al4 Aluminum alloy	Spiral and asymmetrical trapezoid arc oscillation deposition pattern employed allowed the reduction of pores formation from 2.64% to 1.09% and 1.22% respectively.

complicated due to the involvement of several unknown factors, including electromagnetic force (EMF), tension force, gravity, and the weight impact of the droplet. Liang et al. [261] conducted a study to evaluate the dynamic behaviour of metal transfer in the form of droplets under different transfer modalities. They used ANOVA to determine the importance of each parameter involved. The presence of defects and imperfections, such as voids and porosity, in Aluminum-based WAAM components, highlights the need to include statistical analysis in AM research. By controlling the size and positioning of the porosity, it is possible to achieve an optimal structure with excellent quality using this manufacturing technique. Derekar et al. [104] conducted a statistical study using ANOVA to examine the variations in porosity diameter in several specimens fabricated using two distinct metal deposition circumstances, namely pulsed MIG and CMT. The investigation focused on verifying these differences by examining the p-values.

In a study conducted by Naveen Srivinas et al. [262], optimization research was carried out to fabricate a thin plate component using the aluminum-based WAAM technique. The study employed the Grey Relational Analysis (GRA) methodology, which involved the following essential tasks: normalising the experimental data, calculating the grey relational coefficients (GRC), and determining the grey relational grades (GRG) for each run. In addition, this study utilised the L9 OA Taguchi method and ANOVA to minimise the number of trials and examine the effects of various input process variables (factors) - wire feed rate (WFR), gas flow rate, and travel speed - on the output variables (response), specifically the deposited weld bead geometry. These variables were previously suggested by Manikandan et al. [263] for the electrochemical drilling process. The methodology recommended for this study is depicted in Fig. 14. Based on the study conducted, the combination of process parameters with a WFR of 7.5 m/min, a traverse speed (TS) of 0.6 m/min, and a gas flow rate of 18 L/min is determined to be the most optimized for maintaining a high-quality thin plate structure.

Multi-variable process parameters necessitate a unique optimization method in order to enhance productivity. As a result, Lee [19] developed a design for optimizing process parameters in the WAAM technique using a non-parametric method called Gaussian Process Regression (GPR) modelling. This approach accurately calculates minor effects and uncertainties, formulating a unique WAAM optimization model. The model achieves higher productivity standards, improved structural integrity, and higher quality.

In summary, researchers may streamline the process of optimizing WAAM by utilising appropriate statistical analysis methods as tabulated

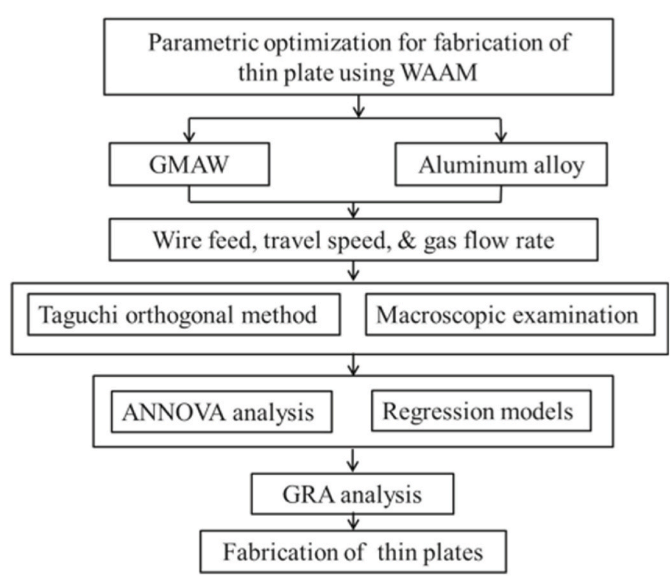

Fig. 14. Proposed research methodology flowchart [262].

in Table 6 which led to enhanced overall WAAM productivity. In order to do this, researchers must endeavour to determine the appropriate process parameter control that has a substantial impact on the result of the desired WAAM structure. Subsequently, an appropriate statistical analysis will be used to minimise errors related to the WAAM process.

5. Recommendations for an optimized WAAM process

WAAM possesses immense potential as the future forefront technology for the additive manufacturing sector. The growing demand for the additive manufacturing (AM) sector, whether for educational or commercial purposes, compelled WAAM technology to develop near-net-shape (NNS) components of superior quality while reducing lead time and capital expenditure. Optimization approaches and innovations are increasingly essential to minimise waste and uphold overall process efficiency. Moreover, implementing optimization techniques has the potential to enhance sustainability by increasing productivity in aiding the economic growth of a nation. Upon conducting a thorough review of the reported study, a radar chart is suggested and developed to establish a correlation between the wire used and the process parameters of the WAAM technique. In addition to the suggested radar chart, a framework for an optimization-based algorithm is proposed.

Table 6
Summary on the characteristics of various analytical optimization methods.

Analytical Optimization Methods	Characteristics	Reference
Taguchi	-Simplify the WAAM process by focusing on reducing the variations of parameters selected. -A robust design to save time and cost whilst improving the quality of deposited structure.	[251,252,262,264,265]
Full Factorial	-Understand how each WAAM process parameter affects the structural quality of deposited parts. -This method considers all possible combinations of each process parameter involved in identifying which have the most significant impact on the WAAM process. -Investigate the interaction of each process parameters with each other.	[65,266–269]
Response Surface Methodology (RSM)	-Simplify the WAAM process by determine the best settings for each process parameter involved while ensuring high quality structure with minimal error. -Utilise mathematical modelling in designing the experiments which is more complex than Taguchi and Full Factorial as it requires high level of expertise to achieve high level of precision in optimizing WAAM process. -Less time and resources needed to execute a precise WAAM optimization.	[70,112,253,256,258–261,270]
Analysis of Variance (ANOVA)	-Identify the important process parameters that affects the deposition. -Quantifying how each process parameter contributes towards the WAAM process. -Employing Design of Experiments (DoE) to collect the response data systematically, such as tensile strength, hardness, etc. -Validating the statistical models obtained for accurate and precise optimization analysis.	[70,112,251–253,256,258–262,264,266,270]
Regression Modelling	-Provide a prediction model on how the changes in process parameters affect the quality of WAAM structure. -Quantifying relationships between each input (process parameters) and output (response). -Quantitatively identifies the significant factors that influenced the overall WAAM performance.	[70,112,256,258–262,266,270]

5.1. Proposed radar chart

By making the appropriate selection between wire material and process parameter using this chart; one can arrive at an optimal decision making for a preliminary WAAM configuration setup specifically for the layer deposition of wall structure application, as seen in Fig. 15. Other application stated in Jafari et al. [271] such as overhang features, crossing feature, corner junction, cylindrical junction, lattice, and struts may also be included as the deposition process parameter employed fall between the proposed range as shown in Fig. 15 and Table 7. The scale depicted on the chart is converted into the specific values of process parameters listed in Table 7. Discovering the most optimal process parameter chosen for a preliminary WAAM configuration is crucial. The WAAM process regulates heat input by selecting proper voltage (V) and/or current (A) values. For bi-metal wire material system, the ideal result may be achieved by combining specific process parameters for each specified material. At the same time, the chart does not specify the precise success rate of a WAAM setup due to factors such as the type of heat source, wire feeding mechanism, and material system; the chosen values can serve as foundations for selecting an optimal process parameters.

5.2. Proposed framework

As depicted in Fig. 16, the framework proposed are applicable to be integrated with any type of material and heat source used. This framework start with the selection of WAAM process parameter and end with performing tests and analysis to procure an ideal properties for the final component in resembling a Near-Net-Shape product. After process parameter selection, three distinct optimization strategies are employed and defects analytical measurement were performed to ensure a successful bead or layer deposition. Then, microstructural characterization and quality control were conducted to identify the structural integrity of the WAAM parts. Proper post processing treatment will be selected for further quality improvement. If the quality improvement were successful, it will proceed to final component properties testing and if it did not meet the required specifications desired, the algorithm will proceed

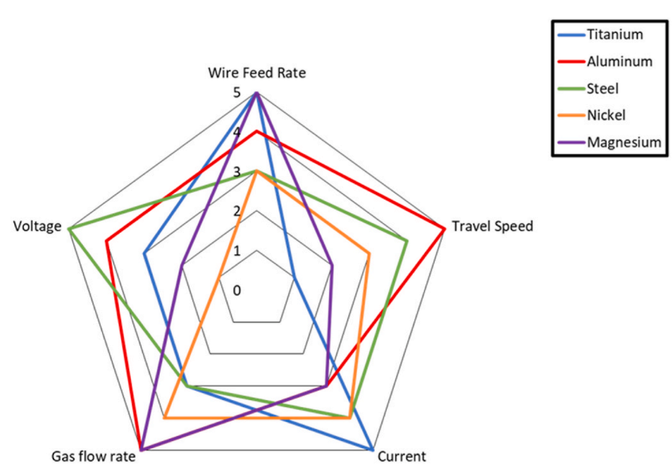

Fig. 15. Proposed optimization correlation chart between type of wire materials and WAAM process parameter.

Table 7
Range of process parameter values correspond towards scale of the correlation chart.

Scale	Wire feed rate (m/min)	Travel speed (m/min)	Voltage (V)	Current (A)	Gas flow rate (L/min)
1	–	0.1–0.6	12–14	–	–
2	–	0.2–0.8	10–17	–	–
3	1–7	0.3–0.8	14–17	70–180	10–20
4	2–8	0.1–1.1	11–19	100–230	15–20
5	1–10	0.3–1.2	14–27	140–350	15–25

to process parameter selection instead.

The algorithm proposed would significantly enhance the optimization of algorithmic systems, leading to significant advancements in the future development of the WAAM optimization process for various materials with complex geometrical characteristics. Optimal filling process algorithm may consist of enhanced slicing 3D CAD model, improved path planning directions, effective process parameters selection procedures, and high-quality bead deposition strategy mechanism. Enhancements may be made to slicing and path planning algorithms by minimising the overall length of the routes, minimising the number of intersections between sub-paths, and minimising the route accessible for certain structural elements. These improvements aim to save time and minimise material waste. Prioritising the ease of integrating the proposed algorithm with current WAAM equipment and its adaptability is prioritised. This would significantly save non-value-added time and facilitate the development of essential elements for industrial adoption.

Utilising configurable algorithms for deposition techniques provides limitless adaptability, enabling the improvement of material quality and WAAM setups under various environmental and process circumstances. Hence, it is imperative to design innovative optimization algorithms that effectively balance the slicing and path planning algorithm, process parameter and heat input choices, material qualities, and complex geometrical aspects to get the optimal result.

6. Future insight of WAAM optimization process

The investigation of various heat sources utilised in the WAAM process is regarded as a critical area of research in the AM industry due to its adaptability in processing a wide range of materials. In the future, it may be possible to incorporate multiple heat sources into a WAAM system configuration to optimize heat distribution, temperature gradient, and various types of thermal cycles, thereby enhancing mechanical performance and microstructure. An extensive comprehension of material attributes results in an optimal process configuration, influencing the selection of optimal process parameters.

Utilising an improved measurement control approach may effectively enhance the structural integrity and quality of WAAM components, serving as a valuable tool for optimization. Moreover, the credibility of the optimization process might be enhanced by integrating diverse approaches to analysis and testing. This encompasses the integration of experimental data and statistical analysis. Using various statistical analysis tools allows for the development of more precise data, which is essential for optimization. In addition, the integration of optimization analysis may effectively save time and cost by eliminating the need for trial-and-error approaches, hence minimising material waste. By incorporating the topology optimization (TO) technique into future WAAM systems, it becomes possible to construct a geometric structure that restructures the lattice parameters to reduce material waste. This restructuring allows for weight reduction without compromising the mechanical properties and quality of the components. In order to efficiently develop resource-feasible optimization processes, it is recommended to utilise advanced simulation computation and mathematical modelling tools such as machine learning, decision science heuristic approach, and process modelling design. These tools are beneficial because they can handle a wide range of potential process combinations.

Integrating several manufacturing methods might improve components' characteristics over time and reduce overall costs by eliminating the difficulties related to WAAM [272]. For instance, the integration of the WAAM and synchronous electromagnetic stirring (EMS) production system enables the enhancement of both grain refinement and tensile shear strength [273]. In addition, using a multi-sensor monitoring system and intelligent control, such as Artificial Intelligence (AI), in the WAAM setup allows for more reliable process optimization by effectively reducing and minimising errors [223]. In order to compensate WAAM manufacturability issues involving complex and inaccessible path geometries with difficult offset control, a method based on a data-driven Artificial Neural Network (ANN) system can be implemented to obtain optimized set of solutions.

7. Conclusion

A comprehensive analysis of the Wire Arc Additive Manufacturing (WAAM) process's optimization process has been effectively presented. The analysis primarily focuses on the selection procedure for process parameters, deposition strategies (including path planning algorithms), and the applicability of statistical analysis tools. By thoroughly examining the material's functionality and the performance characteristics of the WAAM-manufactured components, several suggestions have been put forth to advance and improve the optimization method for producing NNS components that are of superior quality and free from defects. WAAM has consistently demonstrated its superiority as the primary production method and is widely utilised in industrial applications for metal Additive production (AM) technology. This manufacturing technique is characterised by a high deposition rate, making it adaptable and advantageous for monetization and commercialization. The deposition rate employed is determined by two primary parameters: wire feed rate (WFR) and heat input. Various heat sources possess distinct benefits relative to one another. Understanding different materials' varying heat input and process control needs is essential in WAAM. In summary, WAAM is a viable alternative to conventional manufacturing techniques on account of its superior mechanical and microstructural properties and its ability to facilitate applications across multiple disciplines. However, further investigation remains essential and required in order to achieve optimization objectives.

Author contribution

All the authors were ranked according to their contribution to the article.

Funding

This work was supported by the Konsortium Kecemerlangan Penyelidikan Grant Scheme (Large Volume Additive Manufacturing, LVAM) from the Ministry of Higher Education (MOHE) in Malaysia (No. KKP001A-2021) and EU H2020 project, MSCA-RISE-2018 (i-Weld, N. 823786).

Data availability

Not applicable.

Code availability

Not applicable.

Ethics approval

The authors declare that the ethics of this article is approved.

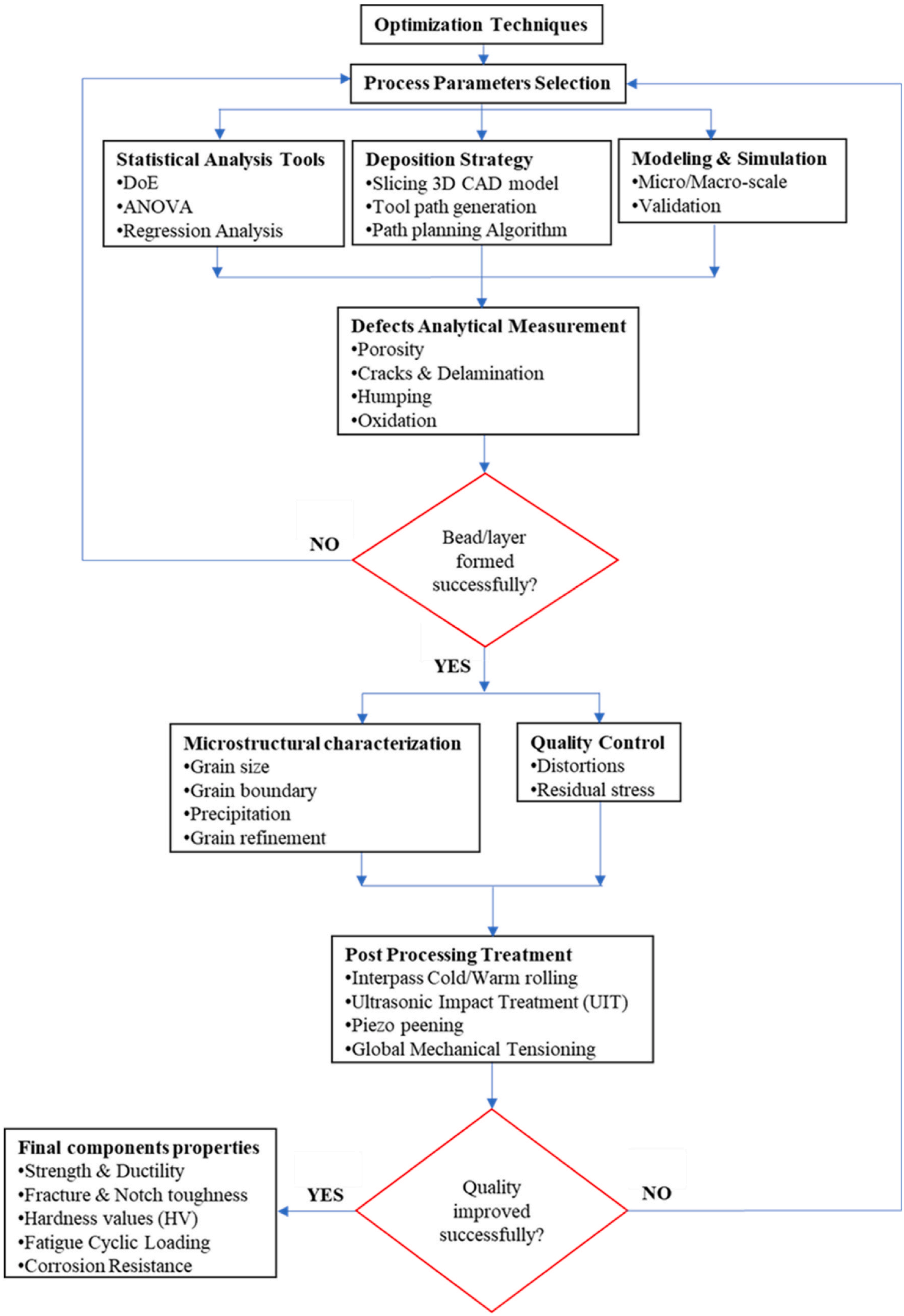

Fig. 16. Optimization-based algorithm framework for optimal WAAM process.

Consent to participate

All the authors agree that the editorial board is qualified to examine the article.

Consent for publication

All the authors agree that the editorial board may publish the article.

Declaration of competing interest

The authors declare that they have no known competing financial interests or personal relationships that could have appeared to influence the work reported in this paper.

Acknowledgements

The Authors would like to acknowledge University of Malaya, Malaysia, and Liverpool John Moore's University (LJMU), United Kingdom (UK), for providing the necessary facilities and resources for this research.

References

[1] Müller J, Grabowski M, Müller C, Hensel J, Unglaub J, Thiele K, Kloft H, Dilger K. Design and parameter identification of wire and arc additively manufactured (WAAM) steel bars for use in construction. Metals 2019;9:725.
[2] Attaran M. The rise of 3-D printing: the advantages of additive manufacturing over traditional manufacturing. Bus Horiz 2017;60:677–88.
[3] Nazan M, Ramli F, Alkahari M, Sudin M, Abdullah M. Process parameter optimization of 3D printer using response surface method. Methodology 2017;15:17.
[4] Rajkumar V, Ajay Vasanth X, Rajesh Kannan A, Siva Shanmugam N. Some studies on optimization of process parameters for wire ARC additive manufacturing of Hastelloy C276 using GRA-GWO hybrid techniques. Proc IME E J Process Mech Eng 2024:09544089241227351.
[5] Ke W, Oliveira J, Cong B, Ao S, Qi Z, Peng B, Zeng Z. Multi-layer deposition mechanism in ultra high-frequency pulsed wire arc additive manufacturing (WAAM) of NiTi shape memory alloys. Addit Manuf 2022;50:102513.
[6] Khodabakhshi F, Farshidianfar M, Bakhshivash S, Gerlich A, Khajepour A. Dissimilar metals deposition by directed energy based on powder-fed laser additive manufacturing. J Manuf Process 2019;43:83–97.
[7] Miao H, Yusof F, Ab Karim MS, Wu B, Raja S, Ibrahim M, Aziz I, Chen D. Interfacial microstructure, element diffusion, mechanical properties and metallurgical bonding mechanism of 316L-AlSi10Mg multi-material parts fabricated by laser powder bed fusion. J Mater Res Technol 2023;26:8351–65.
[8] Adeyemi A, Akinlabi ET, Mahamood RM. Powder bed based laser additive manufacturing process of stainless steel: a review. Mater Today Proc 2018;5:18510–7.
[9] Koepf JA, Gotterbarm MR, Markl M, Körner C. 3D multi-layer grain structure simulation of powder bed fusion additive manufacturing. Acta Mater 2018;152:119–26.
[10] Conde F, Avila J, Oliveira J, Schell N, Oliveira M, Escobar J. Effect of the as-built microstructure on the martensite to austenite transformation in a 18Ni maraging steel after laser-based powder bed fusion. Addit Manuf 2021;46:102122.
[11] Heinl P, Müller L, Körner C, Singer RF, Müller FA. Cellular Ti–6Al–4V structures with interconnected macro porosity for bone implants fabricated by selective electron beam melting. Acta Biomater 2008;4:1536–44.
[12] Bax B, Rajput R, Kellet R, Reisacher M. Systematic evaluation of process parameter maps for laser cladding and directed energy deposition. Addit Manuf 2018;21:487–94.
[13] Li B, Wang L, Wang B, Li D, Oliveira J, Cui R, Yu J, Luo L, Chen R, Su Y. Electron beam freeform fabrication of NiTi shape memory alloys: crystallography, martensitic transformation, and functional response. Mater Sci Eng, A 2022;843:143135.
[14] Rodrigues TA, Bairrão N, Farias FWC, Shamsolhodaei A, Shen J, Zhou N, Maawad E, Schell N, Santos TG, Oliveira JP. Steel-copper functionally graded material produced by twin-wire and arc additive manufacturing (T-WAAM). Mater Des 2022;213:110270.
[15] Li Y, Meng L, Li M, Zhou Y, Liu X, Li X, Zhang G. Allocation and scheduling of deposition paths in a layer for multi-robot coordinated wire and arc additive manufacturing of large-scale parts. Virtual Phys Prototyp 2024;19:e2300680.
[16] Zahidin MR, Yusof F, Rashid SHA, Mansor S, Raja S, Jamaludin MF, Manurung YH, Adenan MS, Hussein NIS. Research challenges, quality control and monitoring strategy for Wire Arc Additive Manufacturing. J Mater Res Technol 2023;24:2769–94.
[17] Huang L, Chen X, Konovalov S, Su C, Fan P, Wang Y, Xiaoming P, Panchenko I. A review of challenges for wire and Arc Additive manufacturing (WAAM). T Indian I Metals 2023;76:1123–39.
[18] Rosli N, Alkahari M, Ramli F, Maidin S, Sudin M, Subramoniam S, Furumoto T. Design and development of a low-cost 3D metal printer. Journal of Mechanical Engineering Research & Developments (JMERD) 2018;41:47–54.
[19] Lee SH. Optimization of cold metal transfer-based wire arc additive manufacturing processes using Gaussian process regression. Metals 2020;10:461.
[20] Ty A, Balcaen Y, Mokhtari M, Alexis J. Influence of deposit and process parameters on microstructure and mechanical properties of Ti6Al4V obtained by DED-W (PAW). J Mater Res Technol 2022;18:2853–69.
[21] Ding D, Pan Z, Cuiuri D, Li H. Wire-feed additive manufacturing of metal components: technologies, developments and future interests. Int J Adv Des Manuf Technol 2015;81:465–81.
[22] Takagi H, Sasahara H, Abe T, Sannomiya H, Nishiyama S, Ohta S, Nakamura K. Material-property evaluation of magnesium alloys fabricated using wire-and-arc-based additive manufacturing. Addit Manuf 2018;24:498–507.
[23] Suárez A, Veiga F, Bhujangrao T, Aldalur E. Study of the mechanical behavior of topologically optimized arc wire direct energy deposition Aerospace fixtures. J Mater Eng Perform 2022:1–13.
[24] Shi J, Li F, Chen S, Zhao Y, Tian H. Effect of in-process active cooling on forming quality and efficiency of tandem GMAW–based additive manufacturing. Int J Adv Des Manuf Technol 2019;101:1349–56.
[25] Del Val AG, Cearsolo X, Suarez A, Veiga F, Altuna I, Ortiz M. Machinability characterization in end milling of Invar36 fabricated by Wire Arc Additive manufacturing. J Mater Res Technol 2023;23:300–15.
[26] Veiga F, Suárez A, Artaza T, Aldalur E. Effect of the heat input on wire-arc additive manufacturing of invar 36 alloy: microstructure and mechanical properties. Weld World 2022;66:1081–91.
[27] Wang J, Zhao Z, Bai P, Zhang R, Zhang Z, Wang L, Du W, Wang F, Huang Z. Microstructure and mechanical properties of AZ31 magnesium alloy prepared using wire arc additive manufacturing. J Alloys Compd 2023;939:168665.
[28] Williams SW, Martina F, Addison AC, Ding J, Pardal G, Colegrove P. Wire+ arc additive manufacturing. Mater Sci Technol 2016;32:641–7.
[29] Gu J, Ding J, Williams SW, Gu H, Bai J, Zhai Y, Ma P. The strengthening effect of inter-layer cold working and post-deposition heat treatment on the additively manufactured Al–6.3 Cu alloy. Mater Sci Eng, A 2016;651:18–26.
[30] Geng Y, Zhao M, Li X, Huang K, Peng X, Zhang B, Fang X, Duan Y, Lu B. Wire-based directed energy deposition of a novel high-performance titanium fiber-reinforced Al5183 Aluminum Alloy. Addit Manuf 2023;65:103445.
[31] Wang Z, Wang J, Lin X, Kang N, Zhang T, Wang Y, Wang L, Dang C, Huang W. Solidification microstructure evolution and its correlations with mechanical properties and damping capacities of Mg-Al-based alloy fabricated using wire and arc additive manufacturing. J Mater Sci Technol 2023;144:28–44.
[32] Wang Z, Bai X, Que M, Zhou X. Wire arc additive manufacturing of network microstructure (TiB+ TiC)/Ti6Al4V composites using flux-cored wires. Ceram Int 2023;49:4168–76.
[33] Shen C, Pan Z, Ma Y, Cuiuri D, Li H. Fabrication of iron-rich Fe–Al intermetallics using the wire-arc additive manufacturing process. Addit Manuf 2015;7:20–6.
[34] Yu B, Chen Z, Wang P, Liu Y, Song X, Dong P. Fatigue and anisotropic behavior of wire-arc additive manufactured TC17 titanium alloy. J Mater Res Technol 2024;28:3463–74.
[35] Wang Z, Wang J, Lin X, Feng L, Ouyang L, Zhang T, Dai C, Yang W, Huang W, Pan F. Microstructure and mechanical properties of a dilute Mg-Gd-Y-Zr alloy fabricated using wire-arc directed energy deposition additive manufacturing. J Mater Res Technol 2024;29:4881–94.
[36] Bai X, Colegrove P, Ding J, Zhou X, Diao C, Bridgeman P, roman Hönnige J, Zhang H, Williams S. Numerical analysis of heat transfer and fluid flow in multilayer deposition of PAW-based wire and arc additive manufacturing. Int J Heat Mass Tran 2018;124:504–16.
[37] Wang L, Zhang Y, Hua X, Shen C, Li F, Huang Y, Ding Y, Zhang P, Lu Q, Zhang T. Twin-wire plasma arc additive manufacturing of the Ti–45Al titanium aluminide: processing, microstructures and mechanical properties. Intermetallics 2021;136:107277.
[38] Josten A, Höfemann M. Arc-welding based additive manufacturing for body reinforcement in automotive engineering. Weld World 2020;64:1449–58.
[39] Le VT, Mai DS, Hoang QH. A study on wire and arc additive manufacturing of low-carbon steel components: process stability, microstructural and mechanical properties. J Braz Soc Mech Sci Eng 2020;42:1–11.
[40] Zhang C, Li Y, Gao M, Zeng X. Wire arc additive manufacturing of Al-6Mg alloy using variable polarity cold metal transfer arc as power source. Mater Sci Eng, A 2018;711:415–23.
[41] Yang J, Ni Y, Li H, Fang X, Lu B. Heat treatment optimization of 2219 aluminum alloy fabricated by wire-Arc Additive manufacturing. Coatings 2023;13:610.
[42] Fang X, Yang J, Jiang X, Li X, Chen R, Huang K. Wire-arc directed energy deposited high-performance AZ31 magnesium alloy via a novel interlayer hammering treatment. Mater Sci Eng, A 2024;889:145864.
[43] Tripathi U, Saini N, Mulik RS, Mahapatra MM. Effect of build direction on the microstructure evolution and their mechanical properties using GTAW based wire arc additive manufacturing. CIRP Journal of Manufacturing Science and Technology 2022;37:103–9.
[44] Navarro M, Matar A, Diltemiz SF, Eshraghi M. Development of a low-cost wire arc additive manufacturing system. Journal of Manufacturing and Materials Processing 2021;6:3.
[45] Ding D, Pan Z, Van Duin S, Li H, Shen C. Fabricating superior NiAl bronze components through wire arc additive manufacturing. Materials 2016;9:652.
[46] He T, Yu S, Shi Y, Huang A. Forming and mechanical properties of wire arc additive manufacture for marine propeller bracket. J Manuf Process 2020;52:96–105.

[47] Xu C, Peng Y, Chen L-Y, Zhang T-Y, He S, Wang K-H. Corrosion behavior of wire-arc additive manufactured and as-cast Ni-Al bronze in 3.5 wt% NaCl solution. Corrosion Sci 2023;215:111048.
[48] Shen C, Pan Z, Ding D, Yuan L, Nie N, Wang Y, Luo D, Cuiuri D, van Duin S, Li H. The influence of post-production heat treatment on the multi-directional properties of nickel-aluminum bronze alloy fabricated using wire-arc additive manufacturing process. Addit Manuf 2018;23:411–21.
[49] Nagamatsu H, Sasahara H, Mitsutake Y, Hamamoto T. Development of a cooperative system for wire and arc additive manufacturing and machining. Addit Manuf 2020;31:100896.
[50] Rodrigues TA, Duarte V, Avila JA, Santos TG, Miranda R, Oliveira J. Wire and arc additive manufacturing of HSLA steel: effect of thermal cycles on microstructure and mechanical properties. Addit Manuf 2019;27:440–50.
[51] Zhou Y, Qin G, Li L, Lu X, Jing R, Xing X, Yang Q. Formability, microstructure and mechanical properties of Ti-6Al-4V deposited by wire and arc additive manufacturing with different deposition paths. Mater Sci Eng, A 2020;772:138654.
[52] Meng Y, Li J, Zhang S, Gao M, Gong M, Chen H. Wire arc additive manufacturing of Ni-Al intermetallic compounds through synchronous wire-powder feeding. J Alloys Compd 2023;943:169152.
[53] Zhang Y, Cheng F, Wu S. Improvement of pitting corrosion resistance of wire arc additive manufactured duplex stainless steel through post-manufacturing heat-treatment. Mater Char 2021;171:110743.
[54] Zhang Y, Cheng F, Wu S. The microstructure and mechanical properties of duplex stainless steel components fabricated via flux-cored wire arc-additive manufacturing. J Manuf Process 2021;69:204–14.
[55] Zhang Y, Wu S, Cheng F. A duplex stainless steel (DSS) with striking tensile strength and corrosion resistance produced through wire arc-additive manufacturing (WAAM) using a newly developed flux-cored wire. Mater Lett 2022;313:131760.
[56] Zhang Y, Wu S, Cheng F. A specially-designed super duplex stainless steel with balanced ferrite: austenite ratio fabricated via flux-cored wire arc additive manufacturing: microstructure evolution, mechanical properties and corrosion resistance. Mater Sci Eng, A 2022;854:143809.
[57] Qi K, Li R, Hu Z, Bi X, Li T, Yue H, Zhang B. Forming appearance analysis of 2205 duplex stainless steel fabricated by cold metal transfer (CMT) based wire and Arc Additive manufacture (WAAM) process. J Mater Eng Perform 2022;31:1–11.
[58] Wu B, Pan Z, Li S, Cuiuri D, Ding D, Li H. The anisotropic corrosion behaviour of wire arc additive manufactured Ti-6Al-4V alloy in 3.5% NaCl solution. Corrosion Sci 2018;137:176–83.
[59] Shao Z, Wu B, Li P, Ma W, Tan H, Li H. Mechanism of corrosion protection in reinforced Ti-6Al-4 V alloy by wire arc additive manufacturing using magnetic arc oscillation. Mater Char 2023:112844.
[60] Yildiz AS, Davut K, Koc B, Yilmaz O. Wire arc additive manufacturing of high-strength low alloy steels: study of process parameters and their influence on the bead geometry and mechanical characteristics. Int J Adv Des Manuf Technol 2020;108:3391–404.
[61] Almeida P, Williams S. Innovative process model of Ti-6Al-4V additive layer manufacturing using cold metal transfer (CMT). In: 2010 international solid freeform fabrication symposium. University of Texas at Austin; 2010.
[62] Kah P. Advancements in intelligent gas Metal Arc Welding systems: fundamentals and applications. Elsevier; 2021.
[63] Wu C, Wang L, Ren W, Zhang X. Plasma arc welding: process, sensing, control and modeling. J Manuf Process 2014;16:74–85.
[64] Wu B, Ding D, Pan Z, Cuiuri D, Li H, Han J, Fei Z. Effects of heat accumulation on the arc characteristics and metal transfer behavior in Wire Arc Additive Manufacturing of Ti6Al4V. J Mater Process Technol 2017;250:304–12.
[65] Dinovitzer M, Chen X, Laliberte J, Huang X, Frei H. Effect of wire and arc additive manufacturing (WAAM) process parameters on bead geometry and microstructure. Addit Manuf 2019;26:138–46.
[66] Wu B, Pan Z, Ding D, Cuiuri D, Li H, Xu J, Norrish J. A review of the wire arc additive manufacturing of metals: properties, defects and quality improvement. J Manuf Process 2018;35:127–39.
[67] Xia C, Pan Z, Polden J, Li H, Xu Y, Chen S, Zhang Y. A review on wire arc additive manufacturing: monitoring, control and a framework of automated system. J Manuf Syst 2020;57:31–45.
[68] Gao W, Zhang Y, Ramanujan D, Ramani K, Chen Y, Williams CB, Wang CC, Shin YC, Zhang S, Zavattieri PD. The status, challenges, and future of additive manufacturing in engineering. Comput Aided Des 2015;69:65–89.
[69] Li Y, Su C, Zhu J. Comprehensive review of wire arc additive manufacturing: hardware system, physical process, monitoring, property characterization, application and future prospects. Results in Engineering 2022;13:100330.
[70] Mai DS, Doan TK, Paris H. Wire and arc additive manufacturing of 308L stainless steel components: optimization of processing parameters and material properties. Engineering Science and Technology, an International Journal 2021;24:1015–26.
[71] Zhang Y, Chen Y, Li P, Male AT. Weld deposition-based rapid prototyping: a preliminary study. J Mater Process Technol 2003;135:347–57.
[72] Zhao H, Zhang G, Yin Z, Wu L. A 3D dynamic analysis of thermal behavior during single-pass multi-layer weld-based rapid prototyping. J Mater Process Technol 2011;211:488–95.
[73] Kazanas P, Deherkar P, Almeida P, Lockett H, Williams S. Fabrication of geometrical features using wire and arc additive manufacture. Proc IME B J Eng Manufact 2012;226:1042–51.
[74] Ding D, Pan ZS, Cuiuri D, Li H. A tool-path generation strategy for wire and arc additive manufacturing. Int J Adv Manuf Technol 2014;73:173–83.
[75] Ding D, Pan Z, Cuiuri D, Li H. A practical path planning methodology for wire and arc additive manufacturing of thin-walled structures. Robot Comput Integrated Manuf 2015;34:8–19.
[76] Pattanayak S, Sahoo SK. Gas metal arc welding based additive manufacturing—a review. CIRP Journal of Manufacturing Science and Technology 2021;33:398–442.
[77] Hamrani A, Bouarab FZ, Agarwal A, Ju K, Akbarzadeh H. Advancements and applications of multiple wire processes in additive manufacturing: a comprehensive systematic review. Virtual Phys Prototyp 2023;18:e2273303.
[78] Srivastava M, Rathee S, Tiwari A, Dongre M. Wire arc additive manufacturing of metals: a review on processes, materials and their behaviour. Mater Chem Phys 2023;294:126988.
[79] Tomar B, Shiva S, Nath T. A review on wire arc additive manufacturing: processing parameters, defects, quality improvement and recent advances. Mater Today Commun 2022;31:103739.
[80] Li K, Chen W, Gong N, Pu H, Luo J, Zhang DZ, Murr LE. A critical review on wire-arc directed energy deposition of high-performance steels. J Mater Res Technol 2023;24:9369–412.
[81] Kumar N, Bhavsar H, Mahesh P, Srivastava AK, Bora BJ, Saxena A, Dixit AR. Wire Arc Additive Manufacturing–A revolutionary method in additive manufacturing. Mater Chem Phys 2022:126144.
[82] Warsi R, Kazmi KH, Chandra M. Mechanical properties of wire and arc additive manufactured component deposited by a CNC controlled GMAW. Mater Today Proc 2022;56:2818–25.
[83] Yuan L, Pan Z, Ding D, Yu Z, van Duin S, Li H, Li W, Norrish J. Fabrication of metallic parts with overhanging structures using the robotic wire arc additive manufacturing. J Manuf Process 2021;63:24–34.
[84] Baffa F, Venturini G, Campatelli G, Galvanetto E. Effect of stepover and torch tilting angle on a repair process using WAAM. Advances in Manufacturing 2022:1–15.
[85] Wang P, Zhang H, Zhu H, Li Q, Feng M. Wire-arc additive manufacturing of AZ31 magnesium alloy fabricated by cold metal transfer heat source: processing, microstructure, and mechanical behavior. J Mater Process Technol 2021;288:116895.
[86] Mok SH, Bi G, Folkes J, Pashby I. Deposition of Ti–6Al–4V using a high power diode laser and wire, Part I: investigation on the process characteristics. Surf Coating Technol 2008;202:3933–9.
[87] Wang C, Suder W, Ding J, Williams S. The effect of wire size on high deposition rate wire and plasma arc additive manufacture of Ti-6Al-4V. J Mater Process Technol 2021;288:116842.
[88] Cao H, Huang R, Yi H, Liu M, Jia L. Asymmetric molten pool morphology in wire-arc directed energy deposition: evolution mechanism and suppression strategy. Addit Manuf 2022:103113.
[89] Xiong J, Lei Y, Chen H, Zhang G. Fabrication of inclined thin-walled parts in multi-layer single-pass GMAW-based additive manufacturing with flat position deposition. J Mater Process Technol 2017;240:397–403.
[90] Evjemo LD, Langelandsvik G, Moe S, Danielsen MH, Gravdahl JT. Wire-arc additive manufacturing of structures with overhang: experimental results depositing material onto fixed substrate. CIRP Journal of Manufacturing Science and Technology 2022;38:186–203.
[91] Wang C, Suder W, Ding J, Williams S. Bead shape control in wire based plasma arc and laser hybrid additive manufacture of Ti-6Al-4V. J Manuf Process 2021;68:1849–59.
[92] Martina F, Mehnen J, Williams SW, Colegrove P, Wang F. Investigation of the benefits of plasma deposition for the additive layer manufacture of Ti–6Al–4V. J Mater Process Technol 2012;212:1377–86.
[93] Ou W, Wei Y, Liu R, Zhao W, Cai J. Determination of the control points for circle and triangle route in wire arc additive manufacturing (WAAM). J Manuf Process 2020;53:84–98.
[94] Singh SR, Khanna P. Wire arc additive manufacturing (WAAM): a new process to shape engineering materials. Mater Today Proc 2021;44:118–28.
[95] Gomez Ortega A, Corona Galvan L, Deschaux-Beaume F, Mezrag B, Rouquette S. Effect of process parameters on the quality of aluminium alloy Al5Si deposits in wire and arc additive manufacturing using a cold metal transfer process. Sci Technol Weld Join 2018;23:316–32.
[96] Zhou Y, Lin X, Kang N, Huang W, Wang J, Wang Z. Influence of travel speed on microstructure and mechanical properties of wire+ arc additively manufactured 2219 aluminum alloy. J Mater Sci Technol 2020;37:143–53.
[97] Wu D, Hua X, Ye D, Li F. Understanding of humping formation and suppression mechanisms using the numerical simulation. Int J Heat Mass Tran 2017;104:634–43.
[98] Yuan L, Pan Z, Ding D, He F, van Duin S, Li H, Li W. Investigation of humping phenomenon for the multi-directional robotic wire and arc additive manufacturing. Robot Comput Integrated Manuf 2020;63:101916.
[99] Wang Z, Zimmer-Chevret S, Léonard F, Abba G. Improvement strategy for the geometric accuracy of bead's beginning and end parts in wire-arc additive manufacturing (WAAM). Int J Adv Des Manuf Technol 2022;118:2139–51.
[100] Yangfan W, Xizhang C, Chuanchu S. Microstructure and mechanical properties of Inconel 625 fabricated by wire-arc additive manufacturing. Surf Coating Technol 2019;374:116–23.
[101] Rosli NA, Alkahari MR, Abdollah MF, Maidin S, Ramli FR. Review on effect of heat input for wire arc additive manufacturing process. J Mater Res Technol 2021;11:2127–45.
[102] Cunningham C, Flynn J, Shokrani A, Dhokia V, Newman S. Invited review article: strategies and processes for high quality wire arc additive manufacturing. Addit Manuf 2018;22:672–86.

[103] Yamaguchi M, Komata R, Furumoto T, Abe S, Hosokawa A. Influence of metal transfer behavior under Ar and CO2 shielding gases on geometry and surface roughness of single and multilayer structures in GMAW-based wire arc additive manufacturing of mild steel. Int J Adv Des Manuf Technol 2022;119:911–26.
[104] Derekar KS, Addison A, Joshi SS, Zhang X, Lawrence J, Xu L, Melton G, Griffiths D. Effect of pulsed metal inert gas (pulsed-MIG) and cold metal transfer (CMT) techniques on hydrogen dissolution in wire arc additive manufacturing (WAAM) of aluminium. Int J Adv Des Manuf Technol 2020;107:311–31.
[105] Xiong J, Zhang G, Zhang W. Forming appearance analysis in multi-layer single-pass GMAW-based additive manufacturing. Int J Adv Des Manuf Technol 2015; 80:1767–76.
[106] Geng H, Li J, Xiong J, Lin X. Optimisation of interpass temperature and heat input for wire and arc additive manufacturing 5A06 aluminium alloy. Sci Technol Weld Join 2017;22:472–83.
[107] Artaza T, Suárez A, Murua M, García J, Tabernero I, Lamikiz A. Wire Arc additive manufacturing of Mn4Ni2CrMo steel: comparison of mechanical and metallographic properties of PAW and GMAW. Procedia Manuf 2019;41:1071–8.
[108] Zhang W, Ding C, Wang H, Meng W, Xu Z, Wang J. The forming profile model for cold metal transfer and plasma wire-arc deposition of nickel-based alloy. J Mater Eng Perform 2021;30:4872–81.
[109] Sahul M, Sahul M, Bočáková B, Kolařík L, Němec T, Kolaříková M. Effect of welding mode on selected properties of additively manufactured AA5087 aluminium alloy parts. In: Journal of physics: conference series. IOP Publishing; 2024, 012017.
[110] Zhang L, Wang S, Wang H, Wang J, Wang T, Dai X. Investigate the effect of arc characteristic on the mechanical properties of 5A56 Al alloy in CMT arc additive manufacturing. CIRP Journal of Manufacturing Science and Technology 2023;40: 102–13.
[111] Zhang L, Wang S, Wang H, Wang J, Bian W. Mechanical properties and microstructure revolution of vibration assisted wire arc additive manufacturing 2319 aluminum alloy. Mater Sci Eng, A 2023;885:145634.
[112] Zhang Z, Yan J, Lu X, Zhang T, Wang H. Optimization of porosity and surface roughness of CMT-P wire arc additive manufacturing of AA2024 using response surface methodology and NSGA-II. J Mater Res Technol 2023;24:6923–41.
[113] Hu Y, Chen F, Cao S, Fan Y, Xie R. Preparation and characterization of CMT wire arc additive manufacturing Al-5% Mg alloy depositions through assisted longitudinal magnetic field. J Manuf Process 2023;101:576–88.
[114] Van D, Dinda G, Park J, Mazumder J, Lee SH. Enhancing hardness of Inconel 718 deposits using the aging effects of cold metal transfer-based additive manufacturing. Mater Sci Eng, A 2020;776:139005.
[115] Fang X, Zhang L, Li H, Li C, Huang K, Lu B. Microstructure evolution and mechanical behavior of 2219 aluminum alloys additively fabricated by the cold metal transfer process. Materials 2018;11:812.
[116] Xu X, Ding J, Ganguly S, Diao C, Williams S. Preliminary investigation of building strategies of maraging steel bulk material using wire+ arc additive manufacture. J Mater Eng Perform 2019;28:594–600.
[117] Manurung YH, Prajadhiana KP, Adenan MS, Awiszus B, Graf M, Haelsig A. Analysis of material property models on WAAM distortion using nonlinear numerical computation and experimental verification with P-GMAW. Arch Civ Mech Eng 2021;21:1–13.
[118] Wu Q, Mukherjee T, Liu C, Lu J, DebRoy T. Residual stresses and distortion in the patterned printing of titanium and nickel alloys. Addit Manuf 2019;29:100808.
[119] Derekar KS, Ahmad B, Zhang X, Joshi SS, Lawrence J, Xu L, Melton G, Addison A. Effects of process variants on residual stresses in Wire Arc Additive manufacturing of aluminum alloy 5183. J Manuf Sci Eng 2022;144.
[120] Wang J, Zhu K, Zhang W, Zhu X, Lu X. Microstructural and defect evolution during WAAM resulting in mechanical property differences for AA5356 component. J Mater Res Technol 2023;22:982–96.
[121] Li R, Wang R, Zhou X, Yan Z, Huang J, Ma C, Liu Y, Zhang H, Ji R. Microstructure and mechanical properties of 2319 aluminum alloy deposited by laser and cold metal transfer hybrid additive manufacturing. J Mater Res Technol 2023;26: 6342–55.
[122] Fang X, Yang J, Wang S, Wang C, Huang K, Li H, Lu B. Additive manufacturing of high performance AZ31 magnesium alloy with full equiaxed grains: microstructure, mechanical property, and electromechanical corrosion performance. J Mater Process Technol 2022;300:117430.
[123] Haden C, Zeng G, Carter III F, Ruhl C, Krick B, Harlow D. Wire and arc additive manufactured steel: tensile and wear properties. Addit Manuf 2017;16:115–23.
[124] Kumar M, Manikandan M. Evaluation of microstructure, residual stress, and mechanical properties in different planes of Wire+ Arc Additive manufactured nickel-based superalloy. Met Mater Int 2022:1–24.
[125] Yang X, Liu J, Wang Z, Lin X, Liu F, Huang W, Liang E. Microstructure and mechanical properties of wire and arc additive manufactured AZ31 magnesium alloy using cold metal transfer process. Mater Sci Eng, A 2020;774:138942.
[126] Guo Y, Pan H, Ren L, Quan G. Microstructure and mechanical properties of wire arc additively manufactured AZ80M magnesium alloy. Mater Lett 2019;247:4–6.
[127] Hu Y, Chen F, Cao S, Fan Y, Xie R. Improvement of microstructure and mechanical properties of CMT wire arc additive manufacturing Al-Si alloy deposition via interlayer coating TiC nanoparticles. Mater Today Commun 2024; 38:107851.
[128] Li C-y, Liu C-m, Tao L, Guo Y-l, Bin L. In-situ preparation of high oxygen content titanium via wire arc additive manufacturing with tunable mechanical properties. T Nonferr Metal Soc 2024;34:171–83.
[129] Guo Y, Quan G, Celikin M, Ren L, Zhan Y, Fan L, Pan H. Effect of heat treatment on the microstructure and mechanical properties of AZ80M magnesium alloy fabricated by wire arc additive manufacturing. J Magnesium Alloys 2022;10: 1930–40.
[130] Eriksson MCF, Lervåg M, Sørensen C, Robertstad A, Brønstad BM, Nyhus B, Aune R, Ren X, Akselsen OM. Additive manufacture of superduplex stainless steel using WAAM. 2018.
[131] Uralde V, Suarez A, Aldalur E, Veiga F, Ballesteros T. Wall fabrication by direct energy deposition (DED) combining mild steel (ER70) and stainless steel (SS 316L): microstructure and mechanical properties. Materials 2022;15:5828.
[132] Guo L, Zhang L, Andersson J, Ojo O. Solidification structures and phases in wire arc additive manufactured C250 maraging steel. Mater Sci Technol 2022:1–9.
[133] Guo X, Li H, Xue P, Pan Z, Xu R, Ni D, Ma Z. Microstructure and mechanical properties of 600 MPa grade ultra-high strength aluminum alloy fabricated by wire-arc additive manufacturing. J Mater Sci Technol 2023;149:56–66.
[134] Singh A, Nath T, Dommeti SG, Sekar S. Bulk fabrication of SS410 material using cold metal transfer-based Wire Arc Additive manufacturing process at optimized parameters: microstructural and property evaluation. Machines 2022;10:1136.
[135] Geng H, Li J, Xiong J, Lin X, Huang D, Zhang F. Formation and improvement of surface waviness for additive manufacturing 5A06 aluminium alloy component with GTAW system. Rapid Prototyp J 2018;24:342–50.
[136] Fu R, Tang S, Lu J, Cui Y, Li Z, Zhang H, Xu T, Chen Z, Liu C. Hot-wire arc additive manufacturing of aluminum alloy with reduced porosity and high deposition rate. Mater Des 2021;199:109370.
[137] Adebayo A, Mehnen J, Tonnellier X. Limiting travel speed in additive layer manufacturing. 2012.
[138] Su C, Chen X, Gao C, Wang Y. Effect of heat input on microstructure and mechanical properties of Al-Mg alloys fabricated by WAAM. Appl Surf Sci 2019; 486:431–40.
[139] Le VT, Mai DS, Bui MC, Wasmer K, Nguyen VA, Dinh DM, Nguyen VC, Vu D. Influences of the process parameter and thermal cycles on the quality of 308L stainless steel walls produced by additive manufacturing utilizing an arc welding source. Weld World 2022;66:1565–80.
[140] Ryan E, Sabin T, Watts J, Whiting M. The influence of build parameters and wire batch on porosity of wire and arc additive manufactured aluminium alloy 2319. J Mater Process Technol 2018;262:577–84.
[141] Wieczorowski M, Pereira A, Carou D, Gapinski B, Ramírez I. Characterization of 5356 aluminum walls produced by Wire Arc Additive manufacturing (WAAM). Materials 2023;16:2570.
[142] Busachi A, Erkoyuncu J, Colegrove P, Martina F, Ding J. Designing a WAAM based manufacturing system for defence applications. Procedia Cirp 2015;37: 48–53.
[143] Geng R, Du J, Wei Z, Xu S, Ma N. Modelling and experimental observation of the deposition geometry and microstructure evolution of aluminum alloy fabricated by wire-arc additive manufacturing. J Manuf Process 2021;64:369–78.
[144] Zhou J, Jia C, Guo M, Chen M, Gao J, Wu C. Investigation of the WAAM processes features based on an indirect arc between two non-consumable electrodes. Vacuum 2021;183:109851.
[145] Ding J, Colegrove P, Mehnen J, Ganguly S, Almeida PS, Wang F, Williams S. Thermo-mechanical analysis of wire and Arc Additive layer manufacturing process on large multi-layer parts. Comput Mater Sci 2011;50:3315–22.
[146] Srivastava S, Garg RK, Sachdeva A, Sharma VS. Distribution of residual stress in Wire-Arc additively manufactured small-scale component: single-versus multi-level heat input. J Manuf Sci Eng 2023;145:021008.
[147] Aldalur E, Suárez A, Veiga F. Metal transfer modes for Wire Arc Additive Manufacturing Al-Mg alloys: influence of heat input in microstructure and porosity. J Mater Process Technol 2021;297:117271.
[148] Kumar P, Singh RKR, Sharma SK. Effect of welding parameters on bead characteristics and mechanical properties of wire and arc additive manufactured inconel 718. Proc IME C J Mech Eng Sci 2022:09544062221133035.
[149] Meng X, Qin G, Zou Z. Investigation of humping defect in high speed gas tungsten arc welding by numerical modelling. Mater Des 2016;94:69–78.
[150] Lervåg M, Sørensen C, Robertstad A, Brønstad BM, Nyhus B, Eriksson M, Aune R, Ren X, Akselsen OM, Bunaziv I. Additive manufacturing with superduplex stainless steel wire by cmt process. Metals 2020;10:272.
[151] Fang X, Zhang L, Chen G, Dang X, Huang K, Wang L, Lu B. Correlations between microstructure characteristics and mechanical properties in 5183 aluminium alloy fabricated by wire-arc additive manufacturing with different arc modes. Materials 2018;11:2075.
[152] Ayarkwa K, Williams SW, Ding J. Assessing the effect of TIG alternating current time cycle on aluminium wire+ arc additive manufacture. Addit Manuf 2017;18: 186–93.
[153] A Hosseini V, Högström M, Hurtig K, Valiente Bermejo MA, Stridh L-E, Karlsson L. Wire-arc additive manufacturing of a duplex stainless steel: thermal cycle analysis and microstructure characterization. Weld World 2019;63:975–87.
[154] Greebmalai J, Warinsiriruk E. Multi-heat input technique for aluminum WAAM using DP-GMAW process. In: AIP conference proceedings. AIP Publishing LLC; 2020, 050001.
[155] Miao Y, Li C, Yin C, Wei C, Lin Z. Joint characteristics of carbon steel bypass-current PAW on additive manufacturing. J Manuf Process 2021;61:408–16.
[156] Zong R, Chen J, Wu C, Padhy GK. Influence of shielding gas on undercutting formation in gas metal arc welding. J Mater Process Technol 2016;234:169–76.
[157] Pouzet S, Peyre P, Gorny C, Castelnau O, Baudin T, Brisset F, Colin C, Gadaud P. Additive layer manufacturing of titanium matrix composites using the direct metal deposition laser process. Mater Sci Eng, A 2016;677:171–81.
[158] Xu X, Ding J, Ganguly S, Diao C, Williams S. Oxide accumulation effects on wire+ arc layer-by-layer additive manufacture process. J Mater Process Technol 2018; 252:739–50.

[159] Arana M, Ukar E, Rodriguez I, Iturrioz A, Alvarez P. Strategies to reduce porosity in Al-Mg WAAM parts and their impact on mechanical properties. Metals 2021; 11:524.
[160] Kim J-D, Kim JW, Cheon JY, Kim Y-D, Ji C. Effect of shielding gases on the wire arc additive manufacturability of 5 Cr–4 Mo tool steel for die casting mold making. Korean Journal of Metals and Materials 2020;58:852–62.
[161] Roy S, Silwal B, Nycz A, Noakes M, Cakmak E, Nandwana P, Yamamoto Y. Investigating the effect of different shielding gas mixtures on microstructure and mechanical properties of 410 stainless steel fabricated via large scale additive manufacturing. Addit Manuf 2021;38:101821.
[162] Deng F, Yang G, Wu B, Qin L, Zheng J, Zhou S. Microstructure and mechanical properties of hybrid-manufactured maraging steel component using 4% nitrogen shielding gas fabricated by wrought-wire Arc Additive manufacturing. Coatings 2022;12:356.
[163] Li S, Zhang L-J, Ning J, Wang X, Zhang G-F, Zhang J-X, Na S-J, Fatemeh B. Comparative study on the microstructures and properties of wire+ arc additively manufactured 5356 aluminium alloy with argon and nitrogen as the shielding gas. Addit Manuf 2020;34:101206.
[164] Ding J, Colegrove P, Martina F, Williams S, Wiktorowicz R, Palt M. Development of a laminar flow local shielding device for wire+ arc additive manufacture. J Mater Process Technol 2015;226:99–105.
[165] Halisch C, Milcke B, Radel T, Rentsch R, Seefeld T. Influence of oxygen content in the shielding gas chamber on mechanical properties and macroscopic structure of Ti-6Al-4V during wire arc additive manufacturing. Int J Adv Des Manuf Technol 2022:1–12.
[166] Silwal B, Nycz A, Masuo CJ, Noakes MW, Marsh D, Vaughan D. An experimental investigation of the effectiveness of Ar-CO2 shielding gas mixture for the wire arc additive process. Int J Adv Des Manuf Technol 2020;108:1285–96.
[167] Costanza G, Sili A, Tata ME. Weldability of austenitic stainless steel by metal arc welding with different shielding gas. Procedia Struct Integr 2016;2:3508–14.
[168] Jurić I, Garašić I, Bušić M, Kožuh Z. Influence of shielding gas composition on structure and mechanical properties of wire and arc additive manufactured Inconel 625. Jom 2019;71:703–8.
[169] Yang G, Deng F, Zhou S, Wu B, Qin L, Zheng J. Influence of shielding gas nitrogen content on the microstructure and mechanical properties of Cu-reinforced maraging steel fabricated by wire arc additive manufacturing. Mater Sci Eng, A 2022;832:142463.
[170] Green TK, Sridharan N, Chen X, Field KG. Effect of N2-and CO2-containing shielding gases on composition modification and carbonitride precipitation in wire arc additive manufactured grade 91 steel. Addit Manuf 2022;56:102854.
[171] Arivazhagan B, Sundaresan S, Kamaraj M. A study on influence of shielding gas composition on toughness of flux-cored arc weld of modified 9Cr–1Mo (P91) steel. J Mater Process Technol 2009;209:5245–53.
[172] Binesh F, Bahrami A, Hebel M, Aidun DK. Preservation of natural phase balance in multi-pass and Wire Arc Additive manufacturing-made duplex stainless steel structures. J Mater Eng Perform 2021;30:2552–65.
[173] Outokumpu, How to weld type 2205 code plus Two® duplex stainless steel, Outokumpu Stainless, Inc.
[174] Lancaster JF. Metallurgy of welding. Elsevier; 1999.
[175] da Silva LJ, Scotti FM, Fernandes DB, Reis RP, Scotti A. Effect of O2 content in argon-based shielding gas on arc wandering in WAAM of aluminum thin walls. CIRP Journal of Manufacturing Science and Technology 2021;32:338–45.
[176] Wu Q, Lu J, Liu C, Fan H, Shi X, Fu J, Ma S. Effect of molten pool size on microstructure and tensile properties of wire arc additive manufacturing of Ti-6Al-4V alloy. Materials 2017;10:749.
[177] Wang L, Zhang Y, Hua X, Shen C, Li F, Huang Y, Ding Y. Fabrication of γ-TiAl intermetallic alloy using the twin-wire plasma arc additive manufacturing process: microstructure evolution and mechanical properties. Mater Sci Eng, A 2021;812:141056.
[178] Ma Y. Fabrication of gamma titanium aluminide alloys by gas tungsten arc welding-based additive layer manufacturing. 2015.
[179] Teng J, Jiang P, Cong Q, Cui X, Nie M, Li X, Zhang Z. A comparison on microstructure features, compression property and wear performance of TC4 and TC11 alloys fabricated by multi-wire arc additive manufacturing. J Mater Res Technol 2024;29:2175–87.
[180] Feng Y, Zhan B, He J, Wang K. The double-wire feed and plasma arc additive manufacturing process for deposition in Cr-Ni stainless steel. J Mater Process Technol 2018;259:206–15.
[181] Wang S, Gu H, Wang W, Li C, Ren L, Wang Z, Zhai Y, Ma P. Study on microstructural and mechanical properties of an Al–Cu–Sn alloy wall deposited by double-wire Arc Additive manufacturing process. Materials 2019;13:73.
[182] Vazquez L, Iturrioz A, Lopez de Uralde P, Alvarez P. Maximising the deposition rate of 5356 aluminium alloy by CMT-twin-based WAAM while reducing segregation-related problems by local IR thermography. Metals 2023;13:1890.
[183] Wang X, Hu Q, Li T, Liu W, Tang D, Hu Z, Liu K. Microstructure and fracture performance of Wire Arc additively manufactured inconel 625 alloy by hot-wire GTAW. Metals 2022;12:510.
[184] Knapp GL, Gussev M, Shyam A, Feldhausen T, Plotkowski A. Microstructure, deformation and fracture mechanisms in Al-4043 alloy produced by laser hot-wire additive manufacturing. Addit Manuf 2022:103150.
[185] Qi Z, Cong B, Qi B, Sun H, Zhao G, Ding J. Microstructure and mechanical properties of double-wire+ arc additively manufactured Al-Cu-Mg alloys. J Mater Process Technol 2018;255:347–53.
[186] Fan S, Guo X, Tang Y, Guo X. Microstructure and mechanical properties of Al-Cu-Mg alloy fabricated by double-wire CMT Arc Additive manufacturing. Metals 2022;12:416.
[187] Somashekara M, Suryakumar S. Studies on dissimilar twin-wire weld-deposition for additive manufacturing applications. T Indian I Metals 2017;70:2123–35.
[188] Sames WJ, List F, Pannala S, Dehoff RR, Babu SS. The metallurgy and processing science of metal additive manufacturing. Int Mater Rev 2016;61:315–60.
[189] Murav'ev V, Krupskii R, Fizulakov R, Demyshev P. Effect of the quality of filler wire on the formation of pores in welding of titanium alloys. Weld Int 2008;22: 853–8.
[190] Ding D, Pan Z, Cuiuri D, Li H, Larkin N. Adaptive path planning for wire-feed additive manufacturing using medial axis transformation. J Clean Prod 2016;133: 942–52.
[191] Cardoso A, Assunção E, Pires I. Study of a hardfacing flux-cored wire for arc directed energy deposition applications. Int J Adv Des Manuf Technol 2022;118: 3431–42.
[192] Singh P, Dutta D. Multi-direction slicing for layered manufacturing. J Comput Inf Sci Eng 2001;1:129–42.
[193] Yang Y, Fuh JY, Loh HT, Wong YS. Multi-orientational deposition to minimize support in the layered manufacturing process. J Manuf Syst 2003;22:116–29.
[194] Ruan J, Sparks TE, Panackal A, Liou FW, Eiamsa-Ard K, Slattery K, Chou H-N, Kinsella M. Automated slicing for a multiaxis metal deposition system. 2007.
[195] Ma G, Zhao G, Li Z, Xiao W. A path planning method for robotic wire and arc additive manufacturing of thin-walled structures with varying thickness. In: IOP conference series: materials science and engineering. IOP Publishing; 2019, 012018.
[196] Zhang J, Wang Q, Xiao G, Zhou J. Filling path planning and polygon operations for Wire Arc Additive manufacturing process. Math Probl Eng 2021:2021.
[197] Dunlavey MR. Efficient polygon-filling algorithms for raster displays. ACM Trans Graph 1983;2:264–73.
[198] McLouth TD, Severino JV, Adams PM, Patel DN, Zaldivar RJ. The impact of print orientation and raster pattern on fracture toughness in additively manufactured ABS. Addit Manuf 2017;18:103–9.
[199] Park SC, Choi BK. Tool-path planning for direction-parallel area milling. Comput Aided Des 2000;32:17–25.
[200] Rajan V, Srinivasan V, Tarabanis KA. The optimal zigzag direction for filling a two-dimensional region. Rapid Prototyp J 2001;7:231–41.
[201] Zhang T, Li H, Gong H, Ding J, Wu Y, Diao C, Zhang X, Williams S. Hybrid wire-arc additive manufacture and effect of rolling process on microstructure and tensile properties of Inconel 718. J Mater Process Technol 2022;299:117361.
[202] Farouki R, Koenig T, Tarabanis K, Korein J, Batchelder J. Path planning with offset curves for layered fabrication processes. J Manuf Syst 1995;14:355–68.
[203] Yang Y, Loh HT, Fuh J, Wang Y. Equidistant path generation for improving scanning efficiency in layered manufacturing. Rapid Prototyp J 2002;8:30–7.
[204] Li H, Dong Z, Vickers GW. Optimal toolpath pattern identification for single island, sculptured part rough machining using fuzzy pattern analysis. Comput Aided Des 1994;26:787–95.
[205] Wang H, Jang P, Stori JA. A metric-based approach to two-dimensional (2D) tool-path optimization for high-speed machining. J Manuf Sci Eng 2005;127:33–48.
[206] Ren F, Sun Y, Guo D. Combined reparameterization-based spiral toolpath generation for five-axis sculptured surface machining. Int J Adv Manuf Technol 2009;40:760–8.
[207] Diourté A, Bugarin F, Bordreuil C, Segonds S. Continuous three-dimensional path planning (CTPP) for complex thin parts with wire arc additive manufacturing. Addit Manuf 2021;37:101622.
[208] Bertoldi M, Yardimci M, Pistor C, Guceri S. Domain decomposition and space filling curves in toolpath planning and generation. 1998 international solid freeform fabrication symposium. 1998.
[209] Wasser T, Jayal AD, Pistor C. Implementation and evaluation of novel buildstyles in fused deposition modeling (FDM). 1999 International Solid Freeform Fabrication Symposium 1999.
[210] Chiu W, Yeung Y, Yu KM. Toolpath generation for layer manufacturing of fractal objects. Rapid Prototyp J 2006;12:214–21.
[211] Jin G, Li WD, Gao L. An adaptive process planning approach of rapid prototyping and manufacturing. Robot Comput Integrated Manuf 2013;29:23–38.
[212] Bi M, Xia L, Tran P, Li Z, Wan Q, Wang L, Shen W, Ma G, Xie YM. Continuous contour-zigzag hybrid toolpath for large format additive manufacturing. Addit Manuf 2022;55:102822.
[213] Zhang J, Xiao G, Peng J, Yu Y, Zhou J. Path generation strategy and Wire Arc Additive manufacturing of large aviation die with complex gradient structure. Materials 2022;15:6115.
[214] Dwivedi R, Kovacevic R. Automated torch path planning using polygon subdivision for solid freeform fabrication based on welding. J Manuf Syst 2004; 23:278–91.
[215] Ding D, Pan Z, Cuiuri D, Li H, Van Duin S, Larkin N. Bead modelling and implementation of adaptive MAT path in wire and arc additive manufacturing. Robot Comput Integrated Manuf 2016;39:32–42.
[216] Blum H. A transformation for extracting new descriptions of shape, Models for the perception of speech and visual form. 1967. p. 362–80.
[217] Kao J-H, Prinz FB. Optimal motion planning for deposition in layered manufacturing. In: International design engineering technical conferences and computers and information in engineering conference. American Society of Mechanical Engineers; 1998. V006T006A018.
[218] Lee Y, Baek J, Kim YM, Park FC. IMAT: the iterative medial Axis transform, computer graphics forum. Wiley Online Library; 2021. p. 162–81.
[219] Ding D, Pan Z, Cuiuri D, Li H. A multi-bead overlapping model for robotic wire and arc additive manufacturing (WAAM). Robot Comput Integrated Manuf 2015; 31:101–10.

[220] Venturini G, Montevecchi F, Scippa A, Campatelli G. Optimization of WAAM deposition patterns for T-crossing features. Procedia CIRP 2016;55:95–100.
[221] Ding D, Shen C, Pan Z, Cuiuri D, Li H, Larkin N, van Duin S. Towards an automated robotic arc-welding-based additive manufacturing system from CAD to finished part. Comput Aided Des 2016;73:66–75.
[222] Nilsiam Y, Sanders P, Pearce JM. Slicer and process improvements for open-source GMAW-based metal 3-D printing. Addit Manuf 2017;18:110–20.
[223] Nguyen L, Buhl J, Bambach M. Decomposition algorithm for tool path planning for wire-arc additive manufacturing. Journal of Machine Engineering 2018;18:95–106.
[224] Hu Z, Qin X, Shao T, Liu H. Understanding and overcoming of abnormity at start and end of the weld bead in additive manufacturing with GMAW. Int J Adv Des Manuf Technol 2018;95:2357–68.
[225] Ma G, Zhao G, Li Z, Yang M, Xiao W. Optimization strategies for robotic additive and subtractive manufacturing of large and high thin-walled aluminum structures. Int J Adv Des Manuf Technol 2019;101:1275–92.
[226] Aldalur E, Veiga F, Suárez A, Bilbao J, Lamikiz A. Analysis of the wall geometry with different strategies for high deposition wire arc additive manufacturing of mild steel. Metals 2020;10:892.
[227] Aldalur E, Veiga F, Suárez A, Bilbao J, Lamikiz A. High deposition wire arc additive manufacturing of mild steel: strategies and heat input effect on microstructure and mechanical properties. J Manuf Process 2020;58:615–26.
[228] Chakkravarthy V, Jerome S. Printability of multiwalled SS 316L by wire arc additive manufacturing route with tunable texture. Mater Lett 2020;260:126981.
[229] Ayarkwa KF, Pinter Z, Eimer E, Williams S, Ding J, Suder W. Effect of the deposition strategy on Al-Cu alloy wire+ arc additive manufacture. 2021.
[230] Pereira A, Carou D, Fenollera M, Prado T, Gapiński B, Wieczorowski M. Experimental study on the manufacturing of steel inclined walls by directed energy deposition based on dimensional and 3D surface roughness measurements. Materials 2022;15:4994.
[231] Rodrigues TA, Farias FWC, Zhang K, Shamsolhodaei A, Shen J, Zhou N, Schell N, Capek J, Polatidis E, Santos TG. Wire and arc additive manufacturing of 316L stainless steel/Inconel 625 functionally graded material: development and characterization. J Mater Res Technol 2022;21:237–51.
[232] Gou J, Wang Z, Hu S, Shen J, Liu Z, Yang C, Bai Y, Lu WF. Effect of cold metal transfer mode on the microstructure and machinability of Ti–6Al–4V alloy fabricated by wire and arc additive manufacturing in ultra-precision machining. J Mater Res Technol 2022;21:1581–94.
[233] Pan Z, Zhang H, Song X, Wang G, Wu C, Liu X. Influence of micro-rolling on the strength and ductility of plasma-arc additively manufactured Ti–6Al–4V alloys. J Mater Res Technol 2022;21:465–73.
[234] Yuan L, Pan Z, Polden J, Ding D, van Duin S, Li H. Integration of a multi-directional wire arc additive manufacturing system with an automated process planning algorithm. Journal of Industrial Information Integration 2022;26:100265.
[235] Oh W-J, Lee C-M, Kim D-H. Prediction of deposition bead geometry in wire arc additive manufacturing using machine learning. J Mater Res Technol 2022;20:4283–96.
[236] Koli Y, Yuvaraj N, Sivanandam A. Vipin, Control of humping phenomenon and analyzing mechanical properties of Al–Si wire-arc additive manufacturing fabricated samples using cold metal transfer process. Proc IME C J Mech Eng Sci 2022;236:984–96.
[237] Arana M, Ukar E, Rodriguez I, Aguilar D, Álvarez P. Influence of deposition strategy and heat treatment on mechanical properties and microstructure of 2319 aluminium WAAM components. Mater Des 2022;221:110974.
[238] Veiga F, Arizmendi M, Suarez A, Bilbao J, Uralde V. Different path strategies for directed energy deposition of crossing intersections from stainless steel SS316L-Si. J Manuf Process 2022;84:953–64.
[239] Ding D, Yuan L, Huang R, Jiang Y, Wang X, Pan Z. Corner path optimization strategy for wire arc additive manufacturing of gap-free shapes. J Manuf Process 2023;85:683–94.
[240] Wei Y, Liu F, Liu F, Yu D, You Q, Huang C, Wang Z, Jiang W, Lin X, Hu X. Effect of arc oscillation on porosity and mechanical properties of 2319 aluminum alloy fabricated by CMT-wire arc additive manufacturing. J Mater Res Technol 2023;24:3477–90.
[241] Vasudevarao B, Natarajan DP, Henderson M, Razdan A. Sensitivity of RP surface finish to process parameter variation 251. 2000 International solid freeform fabrication symposium 2000.
[242] Akande SO. Dimensional accuracy and surface finish optimization of fused deposition modelling parts using desirability function analysis. Int J Eng Res Technol 2015;4:196–202.
[243] Kumar S, Kannan VN, Sankaranarayanan G. Parameter optimization of ABS-M30i parts produced by fused deposition modeling for minimum surface roughness. International Journal of Current Engineering and Technology 2014;3:93–7.
[244] Liao HT, Shie JR. Optimization on selective laser sintering of metallic powder via design of experiments method. Rapid Prototyp J 2007;13:156–62.
[245] Zhu H, Li N, Liu ZJ. The method for the accuracy improvement of STL offset model based on vertex offset. Adv Mater Res 2011;308:1600–3.
[246] Fisher RA. Statistical methods for research workers. Breakthroughs in statistics: methodology and distribution. Springer; 1970. p. 66–70.
[247] Ross PJ. Taguchi techniques for quality engineering: loss function, orthogonal experiments, parameter and tolerance design. 1988.
[248] Biau DJ, Jolles BM, Porcher R. P value and the theory of hypothesis testing: an explanation for new researchers. Clin Orthop Relat Res 2010;468:885–92.
[249] Cleveland WS, Grosse E, Shyu WM. Local regression models, Statistical models in S. Routledge; 2017. p. 309–76.
[250] Harrell Jr FE, Lee KL, Califf RM, Pryor DB, Rosati RA. Regression modelling strategies for improved prognostic prediction. Stat Med 1984;3:143–52.
[251] Rosli NA, Alkahari MR, Ramli FR, Fadzli M. Influence of process parameter on the height deviation of weld bead in Wire Arc. Addit Manuf 2020;10:1165–76.
[252] Zavdoveev A, Pozniakov V, Baudin T, Kim HS, Klochkov I, Motrunich S, Heaton M, Aquier P, Rogante M, Denisenko A. Optimization of the pulsed arc welding parameters for wire arc additive manufacturing in austenitic steel applications. Int J Adv Des Manuf Technol 2022;119:5175–93.
[253] Kumar A, Maji K. Selection of process parameters for near-net shape deposition in wire arc additive manufacturing by genetic algorithm. J Mater Eng Perform 2020;29:3334–52.
[254] Goldberg D. Genetic algorythms in search, optimization and machine learning. Addison-Wesley PC; 1989.
[255] Montgomery DC. Design and analysis of experiments. New York: John Wiley & Sons, Inc.; 2001. p. 200–1. 1997.
[256] Vora J, Parikh N, Chaudhari R, Patel VK, Paramar H, Pimenov DY, Giasin K. Optimization of bead morphology for GMAW-based wire-Arc Additive manufacturing of 2.25 Cr-1.0 Mo steel using metal-cored wires. Appl Sci 2022;12:5060.
[257] Patel VK, Savsani VJ. A multi-objective improved teaching–learning based optimization algorithm (MO-ITLBO). Inf Sci 2016;357:182–200.
[258] Rosli NA, Alkahari MR, Ramli FR, Fadzli bin Abdollah M, Ikhwan Abdul Kudus S, Gazali Herawan S. Parametric optimisation of micro plasma welding for Wire Arc Additive manufacturing by response surface methodology. Manufacturing Technology 2022;22:59–70.
[259] Banerjee S, Paul AR, Mukherjee M, Vadali SRK. A new adaptive process control scheme for efficient wire arc additive manufacturing of thin-walled SS308L component. Int J Adv Des Manuf Technol 2022:1–15.
[260] Gufran M, Mishra A, Singh RK, Sharma AK, Dixit A, Shah A. Dependence of process planning strategy on deposition ratio in wire arc additive manufacturing. Mater Today Proc 2022;62:3468–72.
[261] Liang Z, Jinglong L, Yi L, Jingtao H, Chengyang Z, Jie X, Dong C. Characteristics of metal droplet transfer in wire-arc additive manufacturing of aluminum alloy. Int J Adv Des Manuf Technol 2018;99:1521–30.
[262] Naveen Srinivas M, Vimal K, Manikandan N, Sritharanandh G. Parametric optimization and multiple regression modelling for fabrication of aluminium alloy thin plate using wire arc additive manufacturing. Int J Interact Des Manuf 2022:1–11.
[263] Manikandan N, Kumanan S, Sathiyanarayanan C. Multiple performance optimization of electrochemical drilling of Inconel 625 using Taguchi based grey relational analysis. Engineering Science and Technology, an International Journal 2017;20:662–71.
[264] Wani Z, Abdullah A, Jaafar N, Hussain Z. Multi-stages, multi-responses optimisation of wire arc additive manufacturing parameters using Taguchi method. Mater Today Proc 2022;66:2660–4.
[265] Bhadrakali AS, Sastry DR, Prabhu TR. A hybrid approach consisting of multi-objective and multivariate analyses for WAAM specimens. Engineering Research Express 2023;5:025006.
[266] Chigilipalli BK, Veeramani A. An experimental investigation and neuro-fuzzy modeling to ascertain metal deposition parameters for the wire arc additive manufacturing of Incoloy 825. CIRP Journal of Manufacturing Science and Technology 2022;38:386–400.
[267] Barik S, Bhandari R, Mondal MK. Optimization of Wire Arc Additive manufacturing process parameters for low-carbon steel and properties prediction by support vector regression model. Steel Res Int 2024;95:2300369.
[268] Xia C, Pan Z, Polden J, Li H, Xu Y, Chen S. Modelling and prediction of surface roughness in wire arc additive manufacturing using machine learning. J Intell Manuf 2022:1–16.
[269] Lambiase F, Scipioni SI, Paoletti A. Accurate prediction of the bead geometry in wire arc additive manufacturing process. Int J Adv Des Manuf Technol 2022;119:7629–39.
[270] He S, Zhang Z, Li H, Zhang T, Lu X, Kang J. Multi-objective optimization for forming quality of laser and CMT-P arc hybrid additive manufacturing aluminum alloy using response surface methodology. Actuators, MDPI; 2024. p. 23.
[271] Jafari D, Vaneker TH, Gibson I. Wire and arc additive manufacturing: opportunities and challenges to control the quality and accuracy of manufactured parts. Mater Des 2021;202:109471.
[272] Kapil S, Rajput AS, Sarma R. Hybridization in Wire Arc Additive manufacturing. Front Mech Eng 2022:96.
[273] Zhang J, Di X, Jiang X, Li C. Effect of synchronous electromagnetic stirring on Laves phase morphology and mechanical property of Inconel625-HSLA steel functionally graded material fabricated by wire arc additive manufacturing. Mater Lett 2022;316:132015.

Mr. Muhammad Safwan bin Mohd Mansor is a fellow research student from the Department of Mechanical engineering and a Graduate Research Assistant at Center of Advanced Manufacturing and Materials Processing (AMMP) at the Universiti Malaya. He has completed a BSc and master's degree from the University of Malaya. His research expertise covers the fundamental concept of manufacturing processes and material science prospects. Currently, he is pursuing PhD in the field of wire arc additive manufacturing revolving around duplex stainless steel (DSS).

Dr Sufian Raja is a Post Doctoral Research Fellow in the Department of Mechanical Engineering at the Universiti Malaya. He obtained his PhD degree from the University of Malaya, Malaysia. His resolute research niches are in friction stir welding, friction stir

processing, metal matrix composite and additive manufacturing. He has to his credit one Patent entitled "Controlled Environment Stir Welding (CESW)" (Granted) along with 14 research papers in SCI-Indexed journals, 2 Scopus-indexed conference proceedings and 2 non-indexed conference proceedings. His Google Scholar citation reached up to 260, with 8 H-Index and 5 I10-Index.

Dr Farazila Binti Yusof is an Associate Professor in the Department of Mechanical Engineering at the University of Malaya. She received her PhD degree from the Nagaoka University of Technology, Japan. She previously served as the Head of the Department of Mechanical Engineering, Deputy Dean of the Faculty of Engineering and Head of the Centre of Advanced Manufacturing and Material Processing (AMMP). As it stands now, she holds the position of Director of the Centre for Foundation Studies in Science (PASUM), Universiti Malaya. Her research interests are advanced materials joining (laser welding, friction stir welding, soldering, brazing), powder metallurgy, and additive manufacturing. She has more than 135 research publications in internationally referred journals and conferences to her credit, with an H- index reaching 33. Thus far, she managed to secure several awards and medals, not to mention local and international funds.

Dr Mohd Ridha Muhamad is a Senior Lecturer in the Department of Mechanical Engineering and is the Deputy Head of Advanced Manufacturing and Materials Processing (AMMP) Center at the Universiti Malaya. He obtained Doctor of Engineering from Utsunomiya University Japan in 2015, specializing in magnetic abrasive finishing for superfinishing of tube internal surface for clean environment applications. Prior to his doctoral study, he worked in Yamazaki Mazak Corporation as a Senior Mechanical Design Engineer focusing on CNC prototype machine design and evaluations for mass production. He involved in the design and development of several CNC machines including Quick Turn Nexus series and performed more than 100 variations of cutting conditions such as OD and ID cutting, boring, intermittent cutting, roundness cutting using diamond tool, etc to confirm the machine limits and capabilities. Currently, he is collaborating with Joining Welding Research Institute, Osaka University Japan to develop friction stir welding process in a sustainable way to be implemented in manufacturing industry in Malaysia.

Prof. Dr.-Ing Yupiter HP Manurung is a Full Professor in the School of Mechanical Engineering at Universiti Teknologi MARA (UiTM), Shah Alam, Malaysia. His research activities are mainly focused on simulation and experiment of metal additive manufacturing, generative design, welding technology and Artificial Neural Network.

Dr Mohd Shahriman Adenan is a Senior Lecturer at Universiti Teknologi MARA's School of Mechanical Engineering. Currently serving as the Head of Virtual, Advanced & Additive Manufacturing at the Smart Manufacturing Research Institute (SMRI), his research interests include additive manufacturing design and simulation, as well as surface engineering.

Dr Nur Izan Syahriah Hussein is an Associate Professor in the Faculty of Manufacturing Engineering, at Universiti Teknikal Malaysia Melaka. She holds a PhD in Manufacturing Engineering with a thesis titled 'Direct Method Deposition of Waspaloy Wire Using Laser and Arc Heat Sources' from the University of Nottingham, United Kingdom. She is actively involved in research and development in the Manufacturing Engineering field, especially Welding Technology and Wire and Arc Additive Manufacturing (WAAM). She has written extensively on the topic.

Prof James Ren is a professor of engineering and the director of mechanical engineering and materials research centre in faculty of engineering at Liverpool John Moores University, United Kingdom (UK). He received his PhD and MSc from the University of Hull, United Kingdom in Advanced Materials and Manufacturing Engineering Technology. Currently, he is actively involved in materials science research field especially materials development and processing, the Mechanics of Smart Materials and structures, Computational Mechanics and Applications, Materials Simulation (Physical modelling) and Applications.